

1 Meta-analytical insights into organic matter enrichment in the surface 2 microlayer

3 Amavi N. Silva¹, Surandokht Nikzad^{2,3}, Theresa Barthelmeß¹, Anja Engel¹, Hartmut Herrmann⁴, Manuela
4 van Pinxteren⁴, Kai Wirtz^{3,5}, Oliver Wurl⁶ and Markus Schartau¹

5 ¹GEOMAR Helmholtz Centre for Ocean Research Kiel, Kiel, 24143, Germany

6 ²Trent University, Peterborough, ON K9L 0G2, Canada

7 ³Institute of Coastal Systems, Helmholtz-Zentrum Hereon, Geesthacht, 21502, Germany

8 ⁴Leibniz Institute for Tropospheric Research (TROPOS), Atmospheric Chemistry Department (ACD), Leipzig, 04318,
9 Germany

10 ⁵Christian-Albrechts University of Kiel, Kiel, 24148, Germany

11 ⁶Carl von Ossietzky University of Oldenburg, Oldenburg, 26129, Germany

12 *Correspondence to:* Amavi N. Silva (asilva@geomar.de)

13 **Abstract.** The surface microlayer (SML), the uppermost ~1 mm water layer at the air-water interface, plays a critical role in
14 mediating Earth system processes, yet current knowledge of its composition and organic matter enrichment remains scattered
15 across disciplines. Here, we present the first known meta-analysis of SML studies that quantitatively assesses the distributional
16 characteristics of selected organic compounds, including organic carbon and nitrogen, amino acids, fatty acids, transparent
17 exopolymer particles, carbohydrates, lipids and proteins, through probability density estimates, central tendency metrics and
18 correlations analyses. Our results confirm a preferential enrichment of nitrogen-enriched, particulate organic matter in the
19 SML, while also highlighting the significance of surfactant-specific factors that govern selective enrichment in the SML. We
20 find that enrichment patterns can vary systematically with environmental and methodological conditions, underscoring the
21 need to account for such influences when interpreting observations and developing SML-based models. We provide the full
22 range of typical EF values for the studied compounds, offering a clear reference for assessing whether new measurements are
23 typical or extreme. While delving into the ability of EFs to reflect organic matter partitioning in the SML, we also critically
24 examine their limitations in capturing trophic variability and suggest that EF-based assessments be complemented with metrics
25 that remove background variability from underlying water concentrations, enabling more accurate interpretations of true SML
26 enrichment and informing future modelling efforts. Additionally, our meta-analysis demonstrates that logarithmic data
27 transformations and robust central tendency estimates outperform traditional linear-scale approaches, providing more accurate
28 and reliable SML enrichment estimates.

29 1 Introduction

30 Approximately 70% of the Earth's surface is covered by a hydrated gelatinous 'skin' known as the surface microlayer
31 (hereafter referred to as 'SML'; note that while this term is commonly used to denote the sea surface microlayer, in this study

Formatted: Font colour: Text 2

Deleted: highlighting the significance of compound-specific accumulation and selective enrichment patterns

Deleted: We also observe that the enrichment of a given compound may exhibit notable variability that depends on distinct internal and external conditions.

Formatted: Font colour: Text 2

Deleted: Our evaluation of enrichment factors (EFs) of various measurable compounds provides updated estimates for their typical values and ranges.

Deleted: the

Deleted: of organic matter within

Formatted: Font colour: Text 2

Deleted: conditions

Deleted: . Based on these findings, we propose

Deleted: future SML

Deleted: research should

Deleted: incorporate both

Deleted: absolute concentration changes and enrichment capacities in the SM

Deleted: L

Deleted: alongside their relative changes (as denoted by EFs),

Deleted: to

Deleted: ly

Deleted: ecological implications

Deleted: the value

Deleted: of

Deleted: ,

Deleted: as essential tools for improving the statistical reliability, comparability, and representation of SML enrichment patterns

59 it refers to the surface microlayer in both marine and freshwater systems), which has an operationally defined thickness
 60 typically ranging from 1 – 1000 μm , depending on the sampling method used (i.e., screen, plate, drum; Astrahan *et al.*, 2016;
 61 Hunter, 1980; Liss and Duce, 1997, 1997; Wurl *et al.*, 2009). Situated between the surface waters of all natural water bodies
 62 and the atmosphere, this uppermost multi-component layer (Astrahan *et al.*, 2016; Carlucci *et al.*, 1985; Cunliffe *et al.*, 2013)
 63 creates a unique microhabitat, mainly consisting of neuston (i.e., living communities in the SML), a relatively enriched
 64 complex of organic compounds and strong physico-chemical gradients (Cunliffe *et al.*, 2013; Dietz *et al.*, 1976; Engel and
 65 Galgani, 2016; Hunter and Liss, 1977). The formation and the composition of the SML are governed by a number of biological,
 66 physical and chemical drivers that interact under varying complex environmental conditions and time scales. As a result, the
 67 SML dynamics play a pivotal role in a range of environmental processes such as air-water gas exchange, heat transfer across
 68 boundary layers, biogeochemical cycling, microbial interactions and distribution of pollutants (e.g., Engel *et al.*, 2017; Frew,
 69 1997; Liss and Duce, 1997; Upstill-Goddard, 2006). Therefore, continued investigation of the compositional heterogeneity of
 70 the SML and of the processes therein is crucial to gain deeper insights into its role in ocean biogeochemistry and its potential
 71 climate interactions.

72 The SML is shaped by physical forces: surface tension provides structural stability at the air-water interface (Liss and Duce,
 73 1997), while diffusive fluxes, bubble scavenging and the upward transport of buoyant particles deliver material from
 74 underlying waters, (hereafter referred to as ‘ULW’; Baastrup-Spohr and Staehr, 2009; Chen *et al.*, 2016; Joux *et al.*, 2006;
 75 Obernosterer *et al.*, 2005). In addition, wet and dry atmospheric deposition as well as *in situ* production and degradation also
 76 lead to concentration changes in the SML (Astrahan *et al.*, 2016; Kuznetsova *et al.*, 2004; Milinković *et al.*, 2022). Within the
 77 SML, biological and chemical processes continuously transform compounds between dissolved and particulate forms (Liss
 78 and Duce, 1997), further contributing to its characteristic enrichment relative to the ULW (e.g., Baastrup-Spohr and Staehr,
 79 2009; Gao *et al.*, 2012; Gašparović *et al.*, 2007; Liss and Duce, 1997; Marty and Saliot, 1976; Yang, 1999).

80 Many compounds present in the SML are surface active and are collectively known as ‘surface-active-agents’ or ‘surfactants’
 81 (Maki and Hermansson, 2020; Wurl and Holmes, 2008). Surfactants tend to adsorb at the air-water interface (Wurl *et al.*, 2009)
 82 due to their amphiphilic nature (i.e., presence of both hydrophobic and hydrophilic structural parts; e.g., Marty and Saliot,
 83 1976) and form interfacial films. This leads to modifications of the physico-chemical characteristics of the sea surface, most
 84 notably surface tension, elasticity and viscosity, which alter momentum transfer, micro-scale wave breaking, damping of
 85 capillary waves, ultimately affecting air-sea gas exchange (McKenna and McGillis, 2004; Pereira *et al.*, 2016). Selective
 86 enrichment of surfactants in the SML is strongly influenced by phytoneuston exudation and grazing processes (Kujawinski *et*
 87 *al.*, 2002; Žutić *et al.*, 1981), which release carbohydrates that constitute a major fraction of naturally occurring biosurfactants
 88 (Myklestad, 1995; Penna, 1999). Blooms facilitate the accumulation of large hydrophilic polysaccharides, which can bind to
 89 hydrophobic groups and thereby acquire surfactant properties (Wurl *et al.*, 2011). Surfactant distribution is further shaped by
 90 microbial activity (Hunter and Liss, 1977; Kurata *et al.*, 2016); Baceterioneuston is predominantly lipolytic and proteolytic,

- Deleted: is of a
- Formatted ... [1]
- Deleted: of
- Deleted: (
- Formatted ... [2]
- Formatted ... [3]
- Formatted ... [4]
- Formatted ... [5]
- Formatted ... [6]
- Formatted ... [7]
- Deleted: The primary source of compounds in the SML is th ... [8]
- Deleted: (
- Formatted ... [9]
- Deleted: from where material is transported through diffu ... [11]
- Formatted ... [10]
- Formatted ... [12]
- Formatted ... [13]
- Formatted ... [14]
- Formatted ... [15]
- Formatted ... [16]
- Deleted: Compared to the ULW, the SML is often enrich ... [17]
- Formatted ... [18]
- Formatted ... [19]
- Formatted ... [20]
- Deleted: of these
- Deleted: generally
- Formatted ... [21]
- Deleted: alterations
- Formatted ... [22]
- Deleted: hydrodynamics (i.e., surface tension, turbulent et ... [23]
- Deleted: en
- Deleted:)
- Deleted: suppressing
- Formatted ... [24]
- Formatted ... [25]
- Formatted ... [26]
- Deleted:
- Deleted: form
- Formatted ... [27]
- Formatted ... [28]
- Formatted ... [29]

116 breaking down organic matter (OM) into lipids and proteins (polymers of amino acids; Carlucci *et al.*, 1985; Kjelleberg *et al.*,
117 1976; Sieburth *et al.*, 1976), both of which represent abundant biosurfactant pools in the SML (Brinis *et al.*, 2004; Marty and
118 Saliot, 1976). However, carbohydrates and polysaccharides also constitute major, rapidly utilized substrates for heterotrophic
119 bacteria in the SML (Harvey *et al.*, 1995; Penezić *et al.*, 2022).

120 Surfactants have been categorized according to their solubility into dry and wet surfactants, of which the more insoluble
121 fraction tends to establish as a monolayer at the surface (e.g., phospholipid-like material; Frka *et al.*, 2012), while the adsorption
122 of the latter fraction (more soluble; e.g., proteins and carbohydrates) is governed by concentration-driven equilibria
123 (Asmussen-Schäfer *et al.*, 2026; Laß and Friedrichs, 2011). Nonetheless, the natural soluble surfactant pool frequently reaches
124 a threshold beyond which monolayer-like surfactant coverage of the air-sea interface is observed (Asmussen-Schäfer *et al.*,
125 2026). In addition to their chemical composition, surfactants also vary in their size: Colloidal and particulate organic matter
126 accumulated in the SML further provide substrates to bacterioneuston, thereby helping to stabilize the surface films (Sieburth,
127 1983). The contribution from the particulate pool to the SML's surface activity is estimated to range from 10% to 55%
128 (Gašparović and Čosović, 2003). Furthermore, sticky microgels, like transparent exopolymer particles (TEP) that originate
129 from bacteria and phytoplankton (Allredge *et al.*, 1993), are also found in the SML. Such gel-like particles can form through
130 the coagulation of dissolved polysaccharides (Engel *et al.*, 2004; Mari and Burd, 1998; Schartau *et al.*, 2007), and are capable
131 of incorporating other compounds into a cohesive matrix (Cunliffe *et al.*, 2009; Sieburth, 1983; Wurl and Holmes, 2008),
132 thereby enhancing the structural integrity of surface films (Cunliffe and Murrell, 2009). When the SML becomes highly
133 concentrated in surfactants, these films transform into thick surface slicks that are visible to the naked eye (Liss and Duce,
134 1997). The extent to which OM-driven changes in SML surfactant composition alter air-sea gas exchange remains to be fully
135 understood (Pogorzelski *et al.*, 2006). In addition, inorganic ions, which do not preferentially adsorb at the air-water interface,
136 can be also present in the SML due to passive upward transport (Knipping *et al.*, 2000; Petersen *et al.*, 2004).

137 Liss and Duce (1997) and Pereira *et al.*, (2018) argue that the SML can restrict diffusive fluxes across the air-sea interface,
138 substantially contributing to reduced rates of ocean-atmosphere gas exchange. Surfactants can impact air-sea gas exchange of
139 greenhouse gases such as carbon dioxide (CO₂), methane (CH₄), nitrous oxide (N₂O) and dimethyl sulfide (DMS) (Frew, 1997;
140 Upstill-Goddard, 2006). Asher (1997), from laboratory measurements, and Tsai and Liu (2003), from global ocean
141 observations, estimate a reduction of annual net CO₂ flux by ~20% – 50% due to the presence of the SML, while Wurl *et al.*,
142 (2016), from *in situ* measurements, propose that this decrease can be ~15%. Barthelmeß *et al.* (2021) observed that, in a newly
143 upwelled filament off Mauritania, surfactants can suppress CO₂ gas exchange by 12%. Both lab- and field-based experiments
144 find that natural slicks can reduce air-sea gas exchange by 50 – 60% (Goldman *et al.*, 1988; Salter *et al.*, 2011; Mustafa *et al.*,
145 2020), causing the SML to drive an overall reduction of 19% in the CO₂ fluxes, as shown by *in situ* observations (Mustafa *et al.*
146 *et al.*, 2020). Supporting earlier findings of Springer and Pigford (1970), McKenna and McGillis (2004) and Sabbaghzadeh *et al.*
147 (2017), who raised concerns about the impact of the SML's surfactants on uncertainties in air-sea gas exchange models,

Deleted: . 1

Formatted: Font colour: Text 2

Formatted: Font: Italic, Font colour: Text 2

Formatted: Font colour: Text 2

Formatted: Font: Italic, Font colour: Text 2

Formatted: Font: Italic, Font colour: Text 2

Formatted: Font colour: Text 2

Formatted: Suppress line numbers

Deleted: (

Formatted: Font: Italic

Formatted: Font colour: Text 2

Formatted: Font: Italic, Font colour: Text 2

Formatted: Font colour: Text 2

Formatted: Font colour: Text 2, English (US)

Formatted: Font: Italic, Font colour: Text 2, English (US)

Formatted: Font colour: Text 2, English (US)

Deleted: (Sieburth, 1983) (Gašparović and Čosović, 2003)

Deleted: , so that they reduce surface tension and can form stable interfacial films. (Hunter and Liss, 1977; Kurata *et al.*, 2016) (Carlucci *et al.*, 1985; Kjelleberg *et al.*, 1976; Sieburth *et al.*, 1976)

Formatted: Font colour: Text 2

Formatted: Font colour: Text 2

Formatted: Font colour: Text 2

Deleted: Some of the naturally occurring surfactants in the SML include fatty acids, proteins, certain polysaccharides, humic-like substances and lipids (Brinis *et al.*, 2004; Marty and Saliot, 1976). In

Formatted: Font: Italic

Formatted: Font colour: Text 1

Deleted: (Carlucci *et al.*, 1985; Henrichs and Williams, 1985; Kuznetsova and Lee, 2002; Reinthaler *et al.*, 2008)

Formatted: Font: Italic

159 Mustaffa *et al.* (2020) further argue that conventional wind-based models miscalculate CO₂ exchange up to 20% in areas with
 160 high surfactant concentrations. Moreover, Kock *et al.* (2012) find that, in the eastern tropical North Atlantic region, offsets
 161 between air-sea and diapycnal N₂O fluxes could be explained when surfactant effects were introduced to gas exchange models.
 162 Work of Goldman *et al.*, (1988) find that surfactants in the SML can also suppress air-sea gas exchange of oxygen (O₂).
 163 Disparities in these studies emphasize the significance of accurately assessing the characteristics of the SML and its processes,
 164 as well as integrating this knowledge into climate relevant ocean-atmosphere models (Milinković *et al.*, 2022) in order to
 165 reduce uncertainties in global gas flux estimations, particularly given that SML is seldom included in gas exchange models
 166 (Cen-Lin and Tzung-May, 2013; Engel *et al.*, 2017).

167 Although the composition and the concentration of compounds within the SML are thought to be strongly correlated with those
 168 of the ULW (Basstrup-Spohr and Staehr, 2009; Chen *et al.*, 2016; Joux *et al.*, 2006; Kuznetsova *et al.*, 2004), certain substances
 169 are selectively accumulated at the air-water interface, leading to a pronounced enrichment in the SML. Several studies,
 170 including Carlucci *et al.* (1985), Henrichs and Williams (1985), Kuznetsova and Lee, (2002) and Reinthaler *et al.* (2008), find
 171 stronger enrichment of particulate fractions and nitrogen-based compounds compared to dissolved organic carbon. The
 172 accumulation of these specific compounds in the SML relative to the ULW is often described by the ‘Enrichment Factor’
 173 (hereafter referred to as ‘EF’). The EF of a compound ‘x’ is given by the following concentration ratio:

$$174 \text{ EF of } x = \frac{\text{Concentration of } x \text{ in SML}}{\text{Concentration of } x \text{ in ULW}} \quad (1)$$

175 According to this equation, when the concentration of x is higher in the SML than in the ULW, the EF value rises above 1;
 176 when it is lower, the EF drops below 1, as discussed in Carlson (1983) and Garabetian *et al.* (1993). However, previous studies
 177 report substantial enrichment variability in the SML across environments, compound classes and spatio-temporal scales. For
 178 instance, non-slick areas where microbial degradation processes are dominant can also demonstrate higher EF values,
 179 resembling those found in slick conditions (e.g., Baastrup-Spohr and Staehr, 2009). In contrast, some lakes appear to exhibit
 180 weak SML enrichment even under eutrophic ULW conditions when the waters are concentrated by autochthonous OM (i.e.,
 181 originate within the same ecosystem they are found) that show a lower affinity to the air-water interface (Hillbricht-Ilkowska
 182 and Kostrzewska-Szlakowska, 2004). Freshwater SML tends to be more enriched with organic carbon and nitrogen, total
 183 phosphorous, ammonia and phosphate ions (Knulst *et al.*, 1997; Münster *et al.*, 1998; Södergren, 1987), whereas in marine
 184 environments, carbohydrates, lipids, proteins and amino acids tend to be more enriched (Liss and Duce, 1997). Concentration
 185 variability of the SML can be significantly larger than that of the ULW (Reinthal *et al.*, 2008) though, in some occasions the
 186 two layers show similar variability (Carlson, 1983). Likewise, the extent to which SML composition mirrors the ULW also
 187 varies, with some studies observing tight coupling (e.g., Chen *et al.*, 2016; Joux *et al.*, 2006) and others reporting marked
 188 decoupling linked to different mineralization rates or adsorption dynamics (e.g., Kuznetsova *et al.*, 2004). Differing surface

- Formatted: Font colour: Text 2
- Formatted: Font colour: Text 2
- Formatted: Font colour: Text 2
- Deleted: .
- Formatted: Font: Times New Roman, Not Italic, Font colour: Text 2
- Formatted: Font: Times New Roman, Not Italic, Font colour: Text 2, English (US)
- Deleted: This equation proposes that when the x’s concentration in the SML is higher than that in the ULW, the corresponding EF value becomes > 1 and vice versa
- Deleted: However
- Formatted: Font colour: Text 2
- Deleted: (Reinthal *et al.*, 2008)
- Formatted: Font colour: Text 2

195 activities (i.e., tendency of a substance to accumulate at the interface) of organic compounds is considered a major driver of
196 these transfer dynamics between the SML and the ULW (Engel *et al.*, 2017). Environmental factors further influence SML
197 enrichment, yet their influence remains inconsistent and unresolved (e.g., Baastrup-Spohr and Staehr, 2009; Carlson, 1983;
198 Reinthaler *et al.*, 2008; Sabbaghzadeh *et al.*, 2017). Collectively, these heterogeneous findings highlight the complexity of SML
199 enrichment processes and the need for systematic-cross-study evaluations. These aspects and their implications are further
200 discussed in the Discussion.

201 Overall, the diversity of reported findings highlights the need for a more holistic view of the applicability of EF as a valid and
202 meaningful indicator of compounds enriched in the SML. To address this, we adopted a meta-analysis of existing SML-studies,
203 and conducted a comprehensive analysis to (1) assess OM enrichment in the SML, (2) review current EF estimates and (3)
204 investigate the relevance of EF values as accurate indicators of OM enrichment. The data collection presented here covers
205 mass concentrations of OM compounds and does not include measurements of surface activities or effects on the physico-
206 chemical properties of the uppermost monolayer of the SML. The primary objective is to provide an overview and specific
207 insights into OM compounds that can accumulate within the SML and potentially be linked to biogeochemical processes
208 occurring in the ULW. Accordingly, surfactant measurements of surface activities that have been converted into equivalent
209 surfactant concentrations, such as those expressed as Triton X-100 equivalents, are not considered here. Ultimately, this data
210 compilation, together with the knowledge derived from its initial meta-analysis, is intended to establish a robust foundation
211 for subsequent studies that may support future modelling efforts linking biological processes to functions of the SML and their
212 implications for biogeochemistry and climate.

214 2 Methodology

215 The work presented here synthesizes findings from multiple studies on the SML and employs a quantitative meta-analysis.
216 Meta-analyses provide an essential means of extracting robust and generalizable conclusions by integrating results from
217 fragmented bodies of literature. Such systematic reviews can provide a more precise and accurate understanding of overarching
218 trends, even when individual studies report inconsistent results (Crocetti, 2016). Mengist *et al.* (2020) highlight the importance
219 of meta-analyses by stating that "Systematic reviews with meta-analysis represent the gold standard for conducting reliable
220 and transparent reviews of literature." In fields such as SML research, where methodological diversity is high and
221 environmental variability in inherent, meta-analytical approaches are invaluable in identifying coherent trends and key
222 constraints.

Deleted: (Engel *et al.*, 2017b){Citation}(Engel *et al.*, 2017b)

Formatted: Font: Italic

Formatted: Font colour: Text 2

Formatted: Font colour: Text 2, German

Formatted: Font colour: Text 2

Moved (insertion) [1]

Deleted: (Kuznetsova *et al.*, 2004)when the waters are concentrated by autochthonous OM (i.e., originate within the same ecosystem they are found) that show a lower affinity to the air-water interface(Hillbricht-Ilkowska and Kostrzewska-Szlakowska, 2004). Baastrup-Spohr and Staehr (2009) observed that non-slick areas in which microbial degradation processes are dominant can also (... [30])

Formatted: Suppress line numbers

Moved up [1]: when the waters are concentrated by

Deleted: when the waters are concentrated by autochthonous (... [31])

Deleted: and given the diversity of these results, it is clear that

Formatted: Font colour: Text 2

Deleted: enrichment

Deleted: is warranted

Formatted: Font colour: Text 2

Deleted: ¶ (... [32])

Deleted: ese objectives

Formatted: Font colour: Text 2

Formatted: Font colour: Text 2

Deleted: existing

Deleted: SML

Deleted: New and novel insights gained from these analyses

Deleted: are

Deleted: focused on the

Formatted: Font:

Formatted (... [33])

Formatted: Font colour: Text 2

Deleted: ,

Formatted: Font colour: Text 2

Deleted:

Deleted: ¶

Deleted: ¶

Formatted: Font: Not Italic

273 2.1 Data collection and compilation

274 The primary dataset consists of 2055 data points, extracted from 31 peer-reviewed publications (hereafter referred to as
275 'reference studies') identified through a comprehensive and systematic literature search of scholarly articles published between
276 1967 and 2022. These studies were identified through a structured Google Scholar search conducted between February 2025
277 to April 2025. Search terms included combinations of descriptors related to the surface microlayer (e.g., 'sea surface
278 microlayer', 'SML'), enrichment terminology (e.g., 'enrichment', 'enrichment factor'), and compound specific keywords (e.g.,
279 'surfactants', 'organic carbon', 'organic nitrogen', 'TEP', 'Amino acids', and other organic matter classes). Additional relevant
280 publications were identified through reference lists of retrieved papers. Only datasets providing extractable numerical values
281 were retained.

282 From these studies, directly measured mass concentration data were extracted from simultaneously collected SML and ULW
283 samples (hereafter referred to as $[C]_{SML}$ and $[C]_{ULW}$, respectively) for twelve different observational types of organic
284 compounds (hereafter known as 'target compounds'): total organic carbon (TOC expressed in $mg\ L^{-1}$), particulate organic
285 carbon (POC in $mg\ L^{-1}$), dissolved organic carbon (DOC in $mg\ L^{-1}$), total organic nitrogen (TON in $mg\ L^{-1}$), particulate organic
286 nitrogen (PON in $mg\ L^{-1}$), dissolved organic nitrogen (DON in $mg\ L^{-1}$), amino acids (AA in $\mu mol\ L^{-1}$), fatty acids (FA in μg
287 L^{-1}), transparent exopolymer particles (TEP in $\mu g\ Xeq\ L^{-1}$), carbohydrates (CHO in $\mu mol\ L^{-1}$), lipids (in $\mu mol\ L^{-1}$) and proteins
288 (in $\mu mol\ L^{-1}$). TOC pool includes all forms of organic carbon, thus comprising both POC and DOC. Similarly, the TON pool
289 combines both PON and DON. In general, the particulate pool constitutes a minor fraction of the total pool. The major classes
290 of biopolymers are proteins, CHO and lipids, with AA serving as the monomers of proteins. Depending on the elemental
291 composition of these biopolymers, they contribute to both, the organic carbon and/or organic nitrogen pool. While the ratio of
292 these biopolymers is higher in the particulate pool, it usually declines to only a few percent in the dissolved pool. TEP is
293 composed of polysaccharides (i.e., CHO) with a major fraction contributing to POC, while a minor fraction exists at the
294 interface between the dissolved and particulate phases (Verdugo *et al.*, 2004). These compounds were selected as they represent
295 major carbon and nitrogen pools in the SML, are widely reported across marine and freshwater systems, and are sufficiently
296 represented in the literature to support a robust meta-analytical assessment.

297 The EF values for these target compounds were systematically calculated from corresponding $[C]_{SML} - [C]_{ULW}$ pairs, using Eq.
298 (1). In this study, $[C]_{SML}$, $[C]_{ULW}$ and EF data are collectively referred to as 'primary data'. Auxiliary information associated
299 with the primary data, (i.e., sampling factors and environmental variables) were also extracted when reported and are referred
300 to as 'secondary data'. All analyses were performed using the complete primary data set, independent of whether secondary
301 data were available. The secondary data were summarized only to illustrate existing research gaps in SML studies. All the data,
302 were collected either (1) directly from the source when presented, or else (2) through digitization of graphs and plots using
303 PlotDigitizer (<https://plotdigitizer.com>) and GraphClick v3.0 (<https://graphclick.en.softonic.com/mac>). To estimate

Deleted: 0

Formatted: Font colour: Text 2

Formatted: Font colour: Text 2

Formatted: Suppress line numbers

Deleted: containing

Formatted: Font colour: Text 2

Formatted: Font colour: Text 2

Deleted: concentrations

Deleted: were extracted

Formatted: Font colour: Text 2

Deleted:

Formatted: Font colour: Text 2

Deleted: . They

Formatted: Font colour: Text 2

Formatted: Font colour: Text 2

Deleted: , in general,

Deleted: or, (3) via author correspondence when data was not available in the published materials.

Formatted: Font colour: Text 2

313 digitization uncertainty. TOC data (40 datapoints) from [Baastrup-Spohr and Staehr \(2009\)](#) were digitized five times (200
314 values in total). The standard deviation of repeated measurements was calculated for each point and expressed relative to its
315 average. Across all points, the median relative uncertainty was 0.29%, indicating that digitization introduced minimal error.
316 The resulting compiled database is herein referred to as '[Surface Microlayer Organic Matter Global Data Collection](#)', (SML-
317 *OM*). Supplementary Table S1 provides an overview of the reference studies on which SML-OM is based.

318 2.2 Statistical analyses

319 Given that the SML-OM ranges over several orders of magnitudes, when the dataset is handled in linear-space (i.e. in its
320 original form), higher values dominate and overshadow the features associated with lower values (Feenstra, 2006). These
321 potential limitations of linear scaling were reduced by transforming our primary data into their logarithmic (\log_{10}) counterparts.
322 Hereafter, the term 'linear' refers to the original, untransformed data, while the term 'log' stands for their logarithmic
323 equivalents. The following sections describe the subsequent analyses conducted in our work.

324 2.2.1 Probability distributions

325 Making inferences based on ratios such as EFs requires careful consideration, as changes in the numerator and the denominator
326 often affect these ratios asymmetrically (Keene, 1995). In the context of this study, while reductions in $[C]_{ULW}$ can lead to
327 unusually high EF values that can approach infinity (i.e., stretched towards higher values), increases in $[C]_{ULW}$ may produce
328 EFs decreasing down to 0 (i.e., compressed towards lower values). This results in distributions that significantly deviate from
329 Gaussian (i.e. normally distributed) shape. Therefore, distributional characteristics of the primary data were examined through
330 probability distributions.

331 Probability density functions (hereafter referred to as 'PDF') of the EF values were examined by applying non-parametric
332 Kernel Density Estimates (hereafter referred to as 'KDE'; Parzen, 1962; Silverman, 1986; Wegman, 1972). KDE employs a
333 normalized weighting function – known as 'Gaussian kernel' – which is centered at each datapoint. The sum of these kernels
334 produces a smooth and continuous PDF that fits the underlying data. Selection of the width of a kernel – known as 'bandwidth'
335 – is an integral part of the KDE approach, as bandwidths too small or too large lead to overfitting and underfitting of data,
336 respectively, failing to capture the true patterns in distributions. Following this, optimal bandwidths for linear KDEs were
337 computed based on [Härdle et al. \(2004\)](#). For log KDEs, a fixed bandwidth was applied. Log transformations, unlike the linear
338 scale, produce similar distributions with comparable spreads across variables, allowing a single fixed bandwidth to produce
339 stable and consistent smoothing for all data.

340 Robustness of the KDE method decreases at low sample size. Since the SML-OM contains variables with sample sizes as low
341 as 16 (for proteins), a bootstrap resampling approach was adopted where 67% of the original data (i.e., 2/3 of the sample) were
342 randomly subsampled. This proportion balances the need for sufficient data to generate stable KDEs while still introducing

Deleted: (

Deleted: .

Formatted: Font colour: Text 2

Formatted: Font colour: Text 2

Formatted: Font: Italic, Font colour: Text 1

Formatted: Font: Times New Roman, 10 pt, Not Bold, Italic, Font colour: Text 1, English (US)

Formatted: Font: Italic

Deleted: *Surface Microlayer Data (SMD)*

Deleted: D

Formatted: Font colour: Text 1

Deleted: ¶

Deleted: D

Deleted: optimal

Formatted: Font colour: Text 1

Formatted: Font colour: Text 2

Deleted: .

Formatted: Font colour: Text 2

Deleted: ¶

Deleted: D

Formatted: Font colour: Text 2

Formatted: Font colour: Text 2

Formatted: Font colour: Text 2

353 variability for robustness testing. By allowing consistent treatment across all data types, this approach maintains comparable
354 KDE bandwidth behavior among subsamples. An individual KDE was generated at each iteration. The process was repeated
355 1000 times, each time with a different random subsample, generating a set of KDE. These were then averaged to produce an
356 ensemble mean, from which the final PDFs were derived.

357 Additionally, cumulative distribution functions (hereafter referred to as 'CDF') were determined for [C]_{SML} and [C]_{ULW} from
358 the ensemble means of the bootstrapped KDEs. Appendix A provides further information on the KDE method.

359 2.2.2 Summarization, comparison and correlation estimates of distributions

360 For describing, comparing and relating the resulting PDFs and CDFs, we used standard statistical measures. Their
361 mathematical expressions are given in Appendix B.

- 362 (1) To describe the central tendencies, mode (hereafter referred to as ' x_m '), median (hereafter referred to as ' x '),
363 arithmetic mean (hereafter referred to as ' x_a ') and geometric mean (hereafter referred to as ' x_g '), were computed.
- 364 (2) The values at 5th and 95th percentiles of each distribution (hereafter referred to as 'upper threshold: UT' and 'lower
365 threshold: LT', respectively) were also estimated in order to determine their central 90% range (i.e., degree of spread).
- 366 (3) To numerically compare the [C]_{SML} and [C]_{ULW}, Integrated Quadratic Distance (Hereafter known as 'IQD') values of
367 their CDFs were approximated based on Eq. (B3), which measure how different the two distributions are with regard
368 to symmetry and multimodality.
- 369 (4) To investigate and quantify potential relationships between [C]_{SML} and [C]_{ULW} of each target compound, their linear
370 correlation was analysed by employing both parametric Pearson and non-parametric Spearman's tests (both methods
371 were applied for cross-validation purposes; agreement between the two correlation coefficient values increases the
372 confidence in the robustness of the observed relationship).

373 3 Results

374 Unless otherwise stated, all analyses were performed on log scale. Nevertheless, to avoid potential misinterpretation of log
375 scales in data presentation, primarily due to their limited readability among non-expert audiences (e.g., Menge *et al.*, 2018),
376 all results are presented on linear scale.

377 3.1 Characterizing EF distributions

378 Figure 1 compares the KDE-derived PDFs of the EF values for the carbon-enriched (in blue) and nitrogen-enriched (in orange)
379 organic compounds (Hereafter known as 'PDF_C' and 'PDF_N', respectively). PDF_C was derived from EF values for TOC, DOC,
380 POC, FA, TEP and CHO. The remaining target compounds derive PDF_N. In their linear version (Figure 1(a)), both PDFs

Deleted:) were randomly subsampled and a

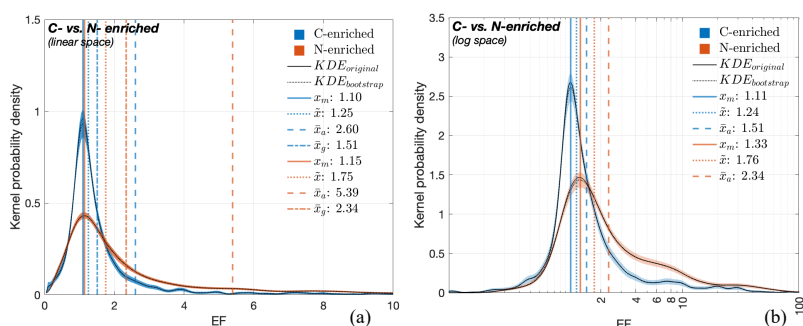
Deleted: ¶

Deleted: ¶

Deleted:

Deleted: (unless otherwise stated)

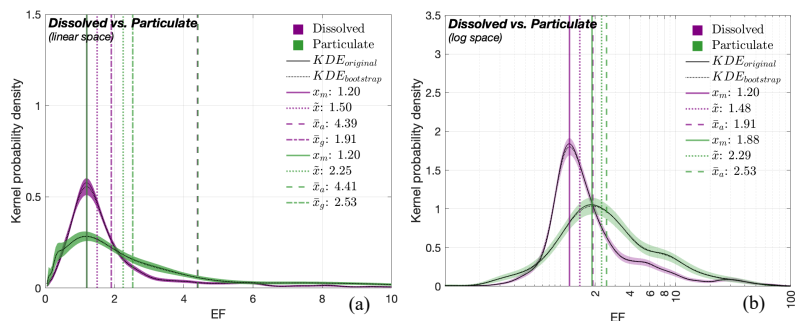
385 demonstrate positive skewness (i.e., right-skewness) with the two x_m values being 1.10 and 1.15, respectively. Nevertheless,
 386 the peak probability density of the PDF_C (i.e., the height of the PDF = ~1) is more than twice that of the PDF_N (~0.4). x of
 387 the two PDFs vary substantially, with PDF_C and PDF_N yielding values of 1.25 and 1.75, respectively. The values for $x_{\bar{a}}$ (2.60
 388 and 5.39, respectively) and $x_{\bar{g}}$ (1.51 and 2.34, respectively) further reflect this divergence. In contrast, their log-transformed
 389 versions (Fig. 1(b)) approximate normal distributions, with PDF_C estimating the (exponentials of) $x_m = 1.11$; $x = 1.24$ and $x_{\bar{a}}$
 390 = 1.51. The PDF_N yields corresponding values of 1.33, 1.76 and 2.34. Their peak probability densities also reflect that the
 391 PDF_C (~2.6) is twice as high as that of PDF_N (~1.5).



392 **Figure 1: PDFs of the EF values for carbon-enriched (blue) and nitrogen-enriched (orange) compounds.** PDFs of the (a) untransformed
 393 (i.e., linear) and (b) log-transformed EF values. The solid black line indicates the KDEs derived from original data while the dashed black
 394 line represents the ensemble mean of bootstrapped KDEs. Central tendency metrics (mode [x_m], median [x], arithmetic mean [$x_{\bar{a}}$], geometric
 395 mean [$x_{\bar{g}}$]) given in panel (b) are the exponentials of the corresponding estimates on the log scale.

396 We also compared EF-based PDFs (Figure 2) for dissolved (PDF_D, in purple) and particulate (PDF_P, in green) OM where we
 397 refer to a filter size of 0.22 μm (Gao *et al.*, 2012). At a linear scale (Figure 2(a)), the PDFs are again right-skewed for the two
 398 clusters, with characteristics: (1) 1.20 (both PDF_D and PDF_P) for x_m ; (2) 1.50 and 2.25 for x ; (3) 4.39 and 4.41 for $x_{\bar{a}}$ and, (4)
 399 1.91 and 2.53 for $x_{\bar{g}}$, respectively. The peak probability density of the PDF_D (~0.6) exceeds that of the PDF_P (~0.3) by nearly
 400 a factor of two. The log PDF_D and PDF_P (Fig. 2(b)) approximate normal distributions alongside the following exponentiated
 401 central values, respectively: (1) $x_m = 1.20$ and 1.88; (2) $x = 1.48$ and 2.29; (3) $x_{\bar{a}} = 1.91$ and 2.53. Their peak probabilities
 402 compare between ~1.8 (for PDF_D) and ~1.0 (for PDF_P).

Formatted: Suppress line numbers



403 **Figure 2:** PDFs of the EF values for dissolved (purple) and particulate (green) compounds. PDFs of (a) linear and (b) log EF values.
 404 See Fig. 1 caption for details on KDEs and central tendency metrics.

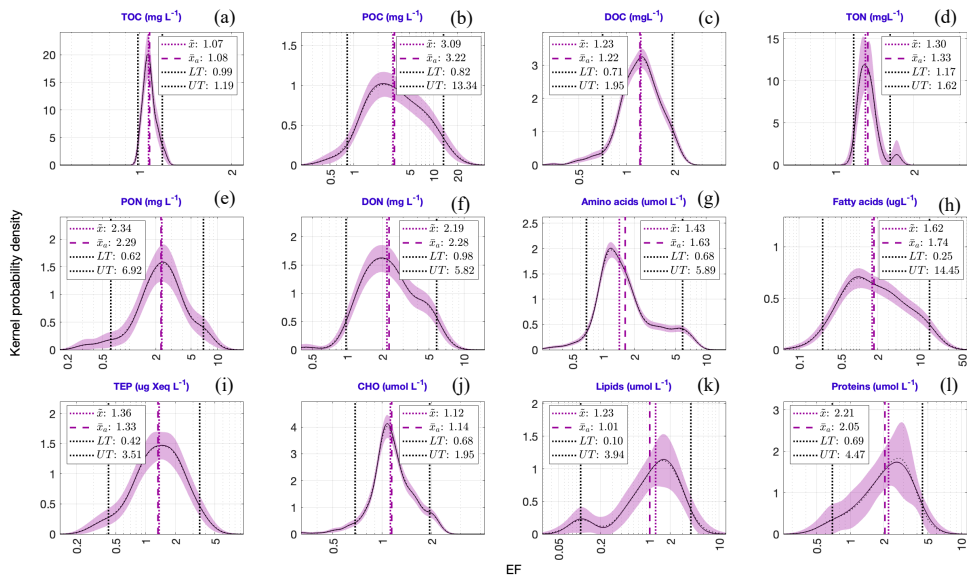
405 Figure 3 displays the PDFs of the EF values for the target compounds. All the distributions exhibit nearly log-normal
 406 characteristics, nevertheless they vary in their degrees of spread. Here, only \hat{x} and \hat{x}_a values estimate the central tendency of
 407 each distribution (the rationale for this approach is discussed in section 4.2). The values of \hat{x} (dotted pink line) and \hat{x}_a (dashed
 408 pink line) are closely aligned in magnitude. According to these derived estimates, median and geometric mean EFs are largest
 409 for POC (Fig. 3(b): $\hat{x} = 3.09$; $\hat{x}_a = 3.22$) across all the target compounds, with PON (Fig. 3(e)) and DON (Fig. 3(f)) following
 410 closely, each exhibiting \hat{x} and \hat{x}_a values > 2 . Although proteins (Fig. 3(l)) also show higher central tendency estimates, it
 411 should be noted that they have the smallest sample size (= 16), followed by lipids (sample size = 20). Therefore, the results of
 412 these two compounds should be interpreted with caution due to their lower statistical robustness. A comparison of threshold
 413 metrics (i.e., LT and UT; see section 2.2.2) reveals that the EF distributions for FA (Fig. 3(h)) and POC (Fig. 3(b)), exhibit the
 414 highest UT values (14.5 and 13.3, respectively) along with the greatest distributional variability. TOC (Fig. 3(a)) and TON
 415 (Fig. 3(d)) show the least variability among all target compounds. While some compounds exhibit well-defined unimodal EF
 416 distributions (e.g., POC, PON), few others (e.g., TON, AA) display polymodal patterns.

417 3.2 Comparing SML and ULW concentrations

418 Figure 4 presents the CDFs of the ULW (in red) and SML (in blue) concentrations for the target compounds. A CDF exhibits
 419 how probability accumulates across a range of values (in the current context, $[C]_{SML}$ and $[C]_{ULW}$ data). All CDFs (both $[C]_{ULW}$
 420 and $[C]_{SML}$) exhibit a characteristic sigmoidal shape: a slow initial rise (i.e., lag phase), followed by a steep rise (i.e.,
 421 exponential phase), eventually reaching a plateau (i.e., stationary phase). CDFs for TOC display two distinctive plateaus
 422 indicating bimodal concentration distributions for both SML and ULW.

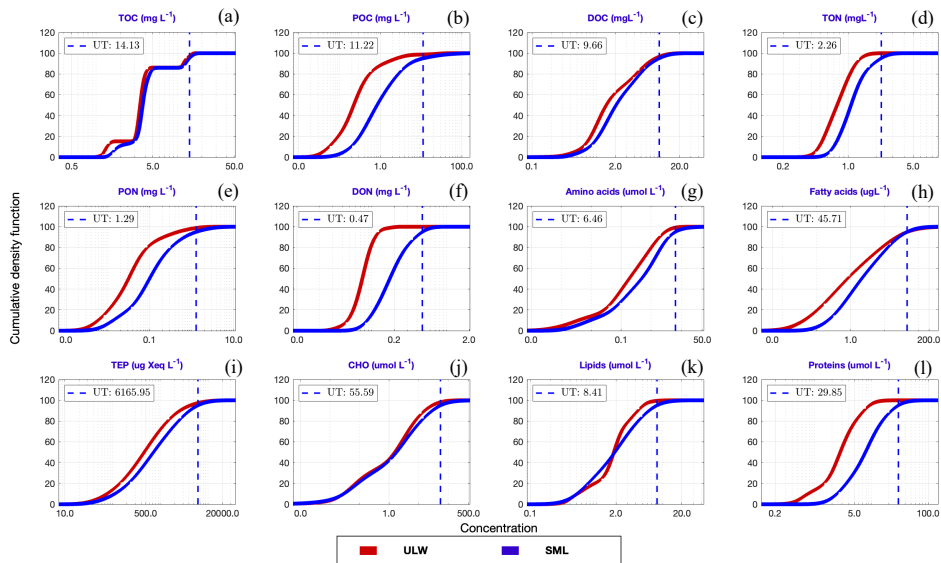
Formatted: Don't suppress line numbers

Deleted: ¶



424 **Figure 3: PDFs of the EF values for the twelve target compounds.** The lower and upper thresholds of each distribution (dashed black
 425 lines) are defined by 5th and 95th percentiles of each PDF (see section 2.2.2). The values of these thresholds, along with the central tendency
 426 metrics given in each panel, are the exponentials of the corresponding estimates in the log space.

427 Additionally, despite the homogeneity in the general shape and trend of these CDFs, their corresponding IQDs (Fig. 5) reveal
 428 that the magnitudes of the offsets between $[C]_{ULW}$ and $[C]_{SML}$ distributions vary substantially across the target compounds.
 429 Lower IQD values indicate greater similarities between the CDFs, while higher values document clear distinguishability and
 430 thus also document a more robust enrichment signal. The lowest IQD is reported for the CDFs of TOC and CHO (0.005) while
 431 that of DON yield the highest in value (0.184). In addition, lower CDFs (i.e. IQD < 0.05) are observed for lipids (0.008), DOC
 432 (0.012), TEP (0.018), AA (0.039) and TON (0.041), whereas POC (0.18) and proteins (0.15) exhibit a greater divergence (i.e.
 433 IQD > 0.15) between $[C]_{ULW}$ and $[C]_{SML}$. The color intensity of each bar reflects the sample size (n) of each target compound
 434 (i.e., smaller the sample, lighter the color).



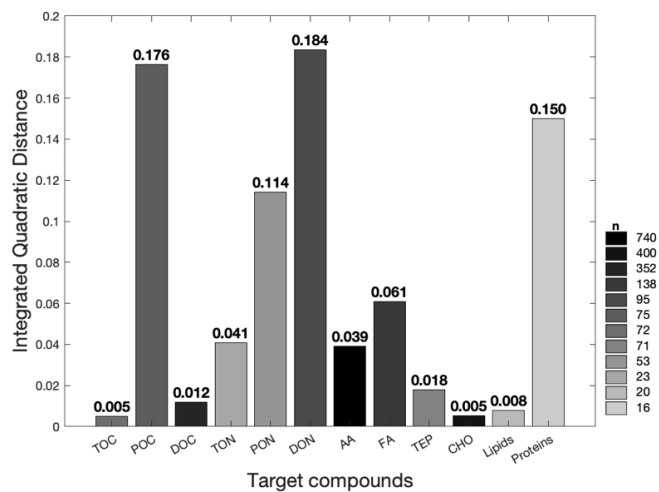
435 **Figure 4: CDFs of the ULW (red) and SML (blue) concentrations for the target compounds.** The upper thresholds for $[C]_{\text{SML}}$ (UT; 436 given by blue dashed lines) are defined by 95th percentiles of the corresponding CDF. The values of these thresholds are the exponentials of 437 the corresponding estimates in the log space. Their corresponding IQDs are given in Figure 5.

438 Correlations between $[C]_{\text{ULW}}$ and $[C]_{\text{SML}}$ of the target compounds were statistically estimated using liner correlation, as 439 presented in Figure 6. The coefficients ‘ ρ ’ and ‘ r ’ stand for the correlation values derived from non-parametric Spearman’s 440 and parametric Pearson correlation tests, respectively. For all target compounds, except for DON, lipids and proteins, we found 441 strong correlations between their SML and ULW concentrations (ρ and $r > 0.5$) with robust positive relationships. Individual 442 datapoints for TOC, DOC and CHO (Figs. 6(a), (c) and (j)) closely fall on the 1:1 reference line where $[C]_{\text{SML}} = [C]_{\text{ULW}}$ (dashed 443 black line). In contrast, those for POC, TON, AA and FA are notably shifted towards the y-axis, suggesting higher $[C]_{\text{SML}}$ 444 values relative to $[C]_{\text{ULW}}$ that corresponds to potentially enriched (depleted) SML (ULW) concentrations against ULW (SML) 445 concentrations (see inset plot in Fig. 6(a)). Although TEP shows a slight enrichment in the SML, the effect is not particularly 446 pronounced (Figure 6(i)). In addition, all the datapoints (regardless of whether they display copulation or not) were further 447 color-coded according to their respective EFs. The results reveal an overall consistency in EFs across concentration ranges

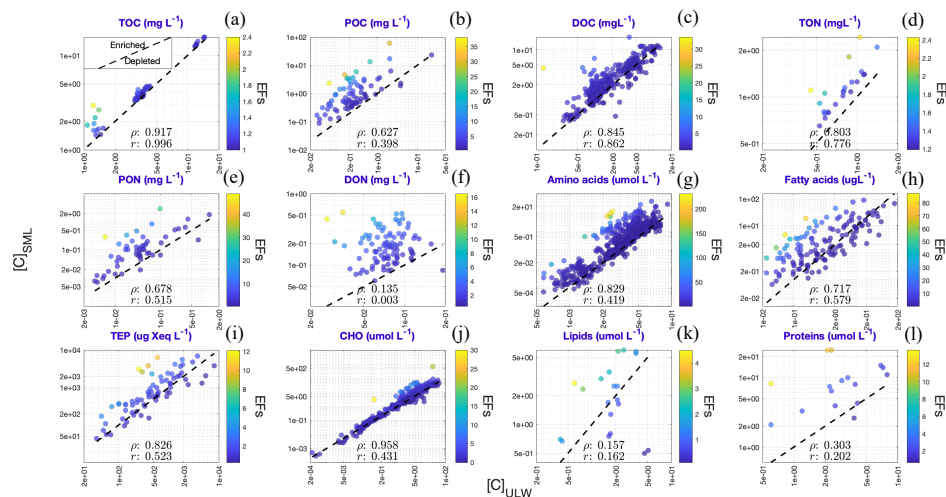
Formatted: Don't suppress line numbers

448 irrespective of their magnitudes. For example, in Fig. 6(c), EF values remain below 5, both when $[C]_{ULW}$ and $[C]_{SML}$ are < 0.5
449 mg L^{-1} and $> 5 \text{ mg L}^{-1}$. This pattern holds across nearly all the target compounds.

Deleted: ¶



450 **Figure 5: IQD values quantifying the divergence between ULW and SML concentrations for each target compound.** The IQD
451 represents the squared difference between ULW- and SML-based CDFs shown in Figure 4. Higher IQD indicates greater divergence between
452 the two distributions and vice versa. Bar color intensity corresponds with the sample sizes.



454 **Figure 6: Linear correlation between $[C]_{ULW}$ and $[C]_{SML}$ for the target compounds.** The datapoints are color-coded based on their
 455 corresponding EFs. Dashed black line indicates 1:1 line when $[C]_{ULW}$ (x-axis) = $[C]_{SML}$ (y-axis). Inset plot in panel (a) exhibits the relevant
 456 implications of the figure: Correlations above the 1:1 line correspond to selective SML enrichment and vice versa. The values of ' ρ ' and ' r '
 457 give Spearman's and Pearson correlation coefficients, respectively.

458 3.3 Investigating concentration-dependent enrichment dynamics

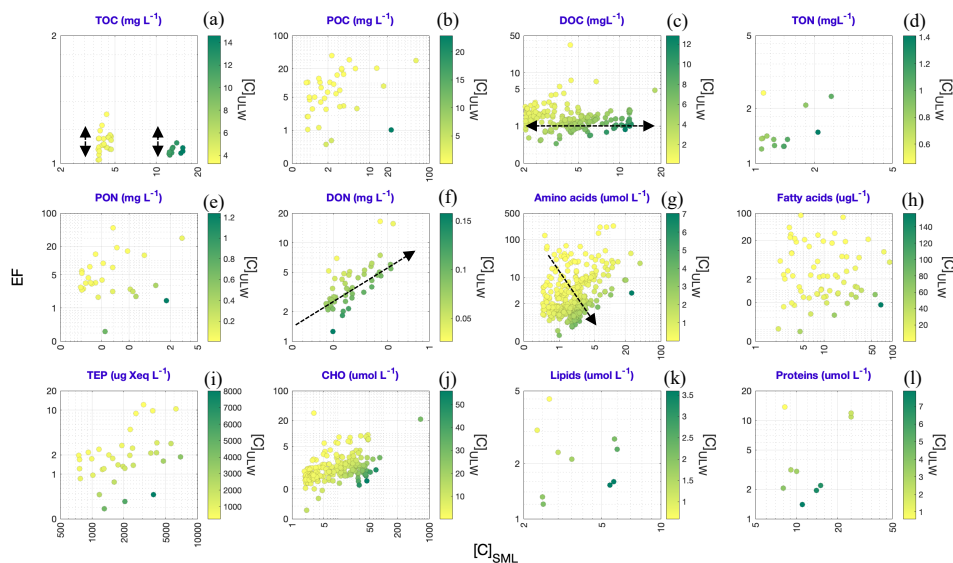
459 Informed by the observations drawn from Fig. 6, Fig. 7 presents a more detailed investigation into the interrelationships among
 460 $[C]_{SML}$, $[C]_{ULW}$ and EFs in the environment. The analysis is restricted to $[C]_{SML}$ values (x-axis) that exceed the x (i.e., median)
 461 of their respective distributions (median is the most stable central tendency metric of a distribution. Discussed further in section
 462 4.2). These elevated $[C]_{SML}$ are compared against the corresponding $[C]_{ULW}$ (color scale) and EF (y-axis) values. The results
 463 reveal following covariation trends:

- 464 (i) TOC reports a generally low range of EF values comparable at both low and high concentrations of SML and
 465 ULW (Fig. 7(a))
- 466 (ii) DOC displays relatively consistent EF values regardless the magnitudes of $[C]_{SML}$ and $[C]_{ULW}$ (Fig. 7(c)), but
 467 also slightly points towards higher EF values in association with low $[C]_{ULW}$
- 468 (iii) DON presents an ascending EF gradient, positively correlated with $[C]_{SML}$ (Fig. 7(f)), revealing more enrichment
 469 to be well reflected in the concentrations found in the SML

470 (iv) AA shows a similar correlation dependence to that of DON, but also reveals a much clearer trend toward higher
471 EF values to be found at lower $[C]_{ULW}$ concentrations (Fig. 7(g))

472 FA (Fig. 7(h)), despite their larger sample sizes, exhibit no clear trend in the $[C]_{SML} - [C]_{ULW} - EF$ triad.

Deleted: fail to display conspicuous consistent trends



473 **Figure 7: Interdependent relationship of $[C]_{SML}$ values with the corresponding $[C]_{ULW}$ and EF values.** The analysis is restricted to
474 $[C]_{SML}$ values that exceed the corresponding α values. The x-axes give the observed $[C]_{SML}$ values against their corresponding EF values on
475 y-axes. Datapoints are color-coded based on corresponding $[C]_{ULW}$ values. The black arrows indicate identified enrichment patterns.

476 4. Discussion

477 A major strength of the SML-OM dataset is its broad coverage of OM concentrations, whereas individual studies are typically
478 restricted to a narrow range of similar ULW conditions. By employing a meta-analytical approach, our study presents the first
479 comprehensive overview of the enrichment dynamics in the SML, based on existing literature. Meta-analytical studies offer a
480 rigorous framework to synthesize evidence across diverse datasets thereby improving the reliability of scientific conclusions.
481 By statistically integrating outcomes from independent investigations, meta-analyses increase overall analytical power, reduce

Formatted: Font colour: Text 2

483 the influence of small-sample variability and, uncover true environmental signals from study-specific biases (i.e., sampling
484 strategies, analytical techniques, spatial scales and seasonality). This not only enhances the generalizability of findings but
485 also exposes gaps and inconsistencies in the existing literature, guiding the development of more robust future studies.

486 In this context, conducting a quantitative assessment of how the reference studies (i.e., those on which the SML-OM is based)
487 are distributed across key domains of SML research provides insights into the most frequently studied aspects (Supplementary
488 Figure S1), thereby explicitly quantifying metadata coverage; research on the SML has increased from about 15 publications
489 per year in the early 2000s to approximately 50 per year by 2016 (Engel *et al.*, 2017). However, our work highlights the
490 potential understudied areas in SML research that call for more in-depth analysis. For instance, majority of the reference studies
491 has been conducted in oceanic and coastal regions (~76% of data) and predominantly during warmer months (~77% of data)
492 with a significant mismatch observed for data collected under low and high wind regimes (~81% vs. 19%, respectively). In
493 light of these research gaps, the following sections interpret the main findings revealed by our analysis and discuss their
494 implications for understanding SML enrichment.

495 4.1 Overarching trends in SML enrichment

496 4.1.1 Generalized enrichment patterns

497 Comparison of KDE-derived PDFs for the EF values of (1) carbon-enriched vs. nitrogen-enriched organic compounds (Fig. 1)
498 and (2) dissolved vs. particulate organic compounds (Fig. 2) yield the following key implications:

- 499 (1) All the estimated original (i.e., linear scale) PDFs (Figs. 1(a) and 2(a)) display higher probability densities for lower
500 EF values and extended tails towards higher EF values (i.e., right-skewness), suggesting that under natural conditions,
501 modest SML enrichment is far more common in general, while extreme enrichment events are rare.
- 502 (2) Nevertheless, variation in the peak probability densities among the PDFs indicate that extreme SML enrichment
503 events are relatively more frequent in nitrogen-enriched compounds (Fig. 1: orange PDF) and particulate forms (Fig.
504 2: green PDF), compared to carbon-enriched compounds (Fig. 1: blue PDF) and dissolved forms (Fig. 2: purple PDF)
- 505 (3) Nitrogen-enriched compounds and particulate forms exhibit a broader EF variability (i.e., higher mode, median, mean
506 values) compared to carbon-enriched compounds and dissolved forms with a relatively more consistent spread (i.e.,
507 lower central tendency metrics)

508 These differences in peaks and central tendency metrics persist in log-transformed PDFs as well (Figs. 1(b) and 2(b)). This
509 validates that these variations are not caused by statistical artifacts but reflect real, natural variability in enrichment behavior.
510 Overall, these findings from our meta-analysis indicate that the OM accumulation in the SML is more effective for (1) nitrogen-
511 enriched than for carbon-enriched compounds and (2) particulate than for dissolved forms. These enrichment patterns likely

Formatted: Font colour: Text 2

Formatted: Font colour: Text 2

Formatted: Font:

Formatted: Suppress line numbers

Deleted: A

Deleted: the distribution of the

Deleted: e studies

Deleted: D

Formatted: Font colour: Text 2

Deleted: ;

Formatted: Font colour: Text 2

Deleted: ve

518 reflect the combined influence of biological, chemical and physical mechanisms acting on the SML. Frka *et al.* (2012) outlined
519 the complex, multicomponent behaviour of the SML, suggesting competitive adsorption of more insoluble surfactants (e.g.,
520 lipid-like material) during highly productive seasons. Selective enrichment of certain polar amino acids (e.g., arginine and
521 glutamic acid) relative to others has been hypothesized (Barthelmeß and Engel, 2022). However, these mechanisms are not
522 yet fully resolved. The molecular structure of N-enriched compounds also promotes aggregation into colloids or microgel
523 particles (Dietz *et al.*, 1976), a process further enhanced by bubble scavenging and low-turbulence trapping (Mopper *et al.*,
524 1995). In contrast, carbon-rich compounds such as polysaccharides are generally more soluble and tend to remain largely
525 distributed in the bulk water, resulting in comparatively lower surface activity and enrichment at the interface (Ćosović and
526 Vojvodić, 1989; Laß *et al.*, 2013). Similarly, particulate OM exists as discrete, larger units, that can be trapped at the interface
527 due to surface tension and by bubble-mediated processes (Robinson *et al.*, 2019). However, some particles, such as TEP
528 ballasted with mineral dust or phytoplankton shells, may sink rather than rise, highlighting the complex balance of forces
529 controlling surface accumulation (Mari *et al.*, 2017). While bubble scavenging represents a process, which can lead to the
530 aggregation of dissolved components (for example, at the rear of rising bubbles; Dukhin *et al.*, 2015; Zhou *et al.*, 1998), a
531 large fraction of dissolved OM, potentially exhibiting reduced overall surface activity, passes through these processes without
532 accumulating at the air–water interface. Transient enrichment of dissolved OM can nonetheless occur. Overall, surface-
533 associated processes such as bubble scavenging and aggregation can enhance the enrichment of particulate compounds in the
534 SML relative to dissolved forms.

535 Our findings contradict some earlier works, including Bastrup-Spohr and Staehr (2009), Liss and Duce (1997), Yang (1999),
536 who suggest that the SML is similarly enriched for both particulate and dissolved organic (and inorganic) compounds, but
537 align with other studies that report opposing results: Dietz *et al.* (1976) provide evidence for enhanced accumulations of
538 particulate matter in the SML through particle aggregation at the surface. The work further links high abundances of living
539 bacteria in the near-surface to higher availability of POC in the SML. Studies of Carlucci *et al.* (1985), Henrichs and Williams,
540 (1985), Kuznetsova *et al.* (2004), Kuznetsova and Lee (2002) and Reinthaler *et al.* (2008) report that POC and PON tend to
541 be more enriched in the SML than DOC. Engel *et al.* (2017) state that the SML has been shown to be enriched in particulate
542 organic matter, particularly in proteinaceous compounds. Together, these findings and our meta-analytical synthesis, indicate
543 that nitrogen-enriched compounds may interfere more critically with interfacial properties. Whether incorporating these
544 nitrogen-based metrics can improve the precision of traditional carbon-only parameterizations of gas exchange suppression
545 (e.g., Barthelmeß *et al.*, 2021; Li *et al.*, 2024) remains an important question for future work.

546 Although nitrogen-enriched compounds seem to exert a strong influence on the SML's interfacial properties at the bulk scale,
547 a compound-specific comparison of three biosurfactants data – AA (Fig. 4(g)), FA (Fig. 4(h)) and CHO (Fig. 4(j)) – reveals a
548 more complex picture (Figure 8): AA, despite their high nitrogen content, does not exhibit the highest enrichment. Instead, its
549 EF values (0.3 - 10) fall between those of CHO (lower end: 0.3 – 2.5) and FA (upper end: 0.1 - 60). Our results are consistent

Deleted: (

Deleted: .

Formatted: Font: Italic

Formatted: Font colour: Text 2

Formatted: Font colour: Text 2

Formatted: Font: Italic, Font colour: Text 2

Formatted: Font colour: Text 2

Formatted: Font: Italic

Deleted: (

Formatted: Font: Italic, English (US)

Formatted: English (US)

Formatted: Font: Italic, English (US)

Formatted: English (US)

Field Code Changed

Deleted: (Dietz *et al.*, 1976)(Mopper *et al.*, 1995)

Formatted: English (US)

Deleted: (Robinson *et al.*, 2019)

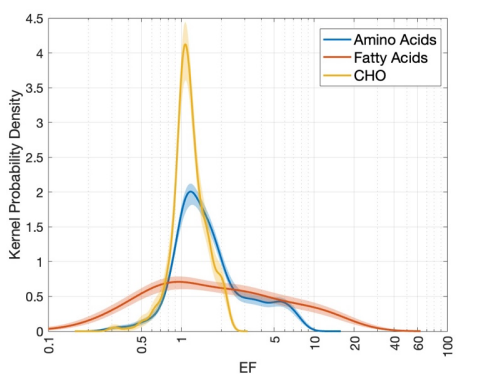
Deleted: M(Mari *et al.*, 2017)a

Deleted: ¶

Formatted: Suppress line numbers

Deleted: range

558 with earlier reports on their natural EF ranges: Polysaccharides can be enriched in the SML up to three-fold compared to the
 559 ULW (Williams *et al.*, 1986; Wurl and Holmes, 2008). Enrichment of AA can vary between 0.3 to 201, depending on their
 560 species-specificity (Cunliffe *et al.*, 2013). This EF hierarchy likely reflects the intermediate surface activity of these three
 561 compounds: (Barthelmeß and Engel, 2022), referring to Čosović and Vojvodić (1998) state that “Lipid-like surfactants exhibit
 562 stronger surface activity, while protein-like, followed by carbohydrate-like, surfactants decrease in activity”. FA dominate
 563 competitive adsorption due to their strong amphiphilic character (i.e., a long hydrophobic tail and small polar head), allowing
 564 them to readily form stable monolayers at the interface. In contrast, proteins are moderately surface-active, while highly soluble
 565 CHO largely remain in the bulk water (Čosović and Vojvodić, 1998; Laß *et al.*, 2013; Laß and Friedrichs, 2011). Consequently,
 566 these patterns suggest that compound-specific enrichment in the SML is driven more by the surfactant properties of individual
 567 compounds than their elemental composition alone. While this hierarchy holds for single-component systems, interactions in
 568 natural SML mixtures are complex, and the structural properties of the nanolayer are influenced by both rare insoluble lipid-
 569 like and abundant soluble carbohydrate-like material. Nevertheless, we do not extend this analysis further as biosurfactants
 570 measurements (1) primarily quantify surface activity rather than enrichment and (2) are subjected to methodological
 571 inconsistencies that limit cross-study comparability. We further acknowledge that the mechanistic links between surfactants,
 572 their behavior and associated ecosystem processes remain incompletely understood.



573 **Figure 8: Comparison of PDFs of the EF values for three bio-surfactants: Amino acids (blue), fatty acids (orange) and carbohydrates**
 574 **(yellow). The figure synthesizes the KDEs given in Figs. 3(g), (h) and (j).**

575 Overall, these overarching trends of SML enrichment underscore the importance of resolving compound-specific accumulation
 576 in the SML, while distinguishing between selective and non-selective enrichment. Cumulative probability comparison results

- Formatted: Font: Italic
- Deleted: (Cunliffe et al., 2013b)
- Formatted: Font: Italic
- Deleted: (
- Deleted: .
- Formatted: Font: Font colour: Text 2, English (US)
- Formatted: Font: (Default) Times New Roman, 10 pt, Font colour: Text 2, English (US)
- Formatted: Font: (Default) Times New Roman, 10 pt, Font colour: Text 2, English (US)
- Formatted: Font: (Default) Times New Roman, 10 pt, Font colour: Text 2, English (US)
- Formatted: Font: (Default) Times New Roman, 10 pt, Font colour: Text 2, English (US)
- Formatted: Font: (Default) Times New Roman, 10 pt, Font colour: Text 2, English (US)
- Formatted: Font: (Default) Times New Roman, 10 pt, Font colour: Text 2, English (US)
- Formatted: Font colour: Text 2
- Formatted: Font: Italic, Font colour: Text 2
- Formatted: Font colour: Text 2
- Formatted
- Formatted
- Formatted: Suppress line numbers
- Formatted: Font colour: Text 2
- Formatted: Font colour: Text 2
- Formatted: Font: Bold, Font colour: Text 2
- Formatted: Font: Bold, Font colour: Text 2
- Formatted: Font: Bold, Font colour: Text 2
- Formatted: Font colour: Text 2
- Formatted: Font: Bold, Font colour: Text 2
- Formatted: Font colour: Text 2, English (US)
- Formatted: Suppress line numbers
- Deleted: These disparities, highlight potential uncertainty
- Formatted: German

585 for the $[C]_{ULW}$ and $[C]_{SML}$ (Figs. 4 and 5) and their corresponding linear correlations (Fig. 6) provide a meta-analytical
586 perspective on how compounds are distributed and accumulated between the two compartments. Here, results concerning
587 lipids and proteins are excluded due to apparent randomness in their distributions, potentially caused by smaller sample sizes.

588 4.1.2 Compound-specific enrichment patterns

589 Significant correlations between $[C]_{ULW}$ and $[C]_{SML}$ of nearly all the target compounds (ρ and $r > 0.5$) are consistent with the
590 overall understanding that the SML's composition is linked to the availability of material in the underlying sub-surface waters
591 (Chen *et al.*, 2016; Joux *et al.*, 2006; Kuznetsova *et al.*, 2004). Contrary to this general pattern, Kuznetsova *et al.* (2004)
592 suggest that certain OM fractions in the SML and ULW may show lack of correlation, potentially due to constraints such as
593 varying mineralization rates between the two layers and surface adsorption processes. Consistent with this view, linear
594 correlation results for DON indicate such decoupling (Fig. 6(f)), though the underlying causes remain unexplored in this study.

595 Early works, also suggested that the variations in the SML concentrations are typically larger than those in the ULW (Reinthal
596 *et al.*, 2008). In agreement, CDFs of the $[C]_{ULW}$ and $[C]_{SML}$ demonstrate faster probability accumulation for ULW than SML
597 (Fig. 4), implying generally smaller magnitudes and lower variability in ULW concentrations compared to SML
598 concentrations. Conversely, Carlson (1983) argues that, in certain occasions, OM variability in the SML and ULW may not
599 significantly differ across temporal and spatial scales. The CDFs for TOC, DOC, TEP and CHO which exhibit the lowest IQD
600 values (Fig. 5), support this but is contradicted by those of the other compounds, with higher IQD values (indicating substantial
601 differences between the two concentrations).

602 Works of Hunter and Liss (1977) and Kurata *et al.* (2016) discuss the selective enrichment of surfactants in the SML, mainly
603 driven by microbial processes. Hydrophobic compounds tend to show more affinity to the surface compared to hydrophilic
604 substances (Marty and Saliot, 1976). In agreement, our linear correlation results reveal preferential accumulation of the
605 biosurfactants, AA (Fig. 6(g)) and FA (Fig. 6(h)), in the SML. Linear correlation results shown in Fig. 6(i) provide evidence
606 to the view that TEP is generally enriched in the SML compared to the ULW (Cunliffe and Murrell, 2009; Cunliffe *et al.*,
607 2009; Wurl and Holmes, 2008), although this enrichment is not strongly pronounced in our dataset. Additionally, the nearly
608 overlapping CDFs for TEP in SML and ULW (Fig. 4(i)) along with its low IQD value ($= 0.081$; Fig. 5) indicate a surprisingly
609 weak enrichment, contrary to expectations. Nevertheless, concentration trend of TEP observed in our data closely aligns with
610 that of CHO (Figs. 4(j) and 5), supporting the prevailing hypothesis that TEP is formed through coagulation of dissolved
611 polysaccharides (Passow, 2000). Thornton *et al.* (2016) observe that TEP and dissolved polysaccharides do not always exhibit
612 significant enrichment in the SML as anticipated.

613 POC and PON correlation patterns (Figs. 6(b) and 6(e), respectively) where $[C]_{SML}$ significantly exceed $[C]_{ULW}$, and that of
614 DOC (Fig. 6(c)) where $[C]_{SML}$ is nearly equal to $[C]_{ULW}$, provide strong meta-analytical evidence to earlier works that discuss
615 the selective enrichment of POC and PON in the SML over DOC (e.g., Carlucci *et al.*, 1992; Henrichs and Williams, 1985;

Deleted: studies

Formatted: Font: English (US)

Formatted: Font colour: Text 2

Deleted: , often parts of biosurfactants (e.g., lipopeptides or polypeptides)...

Deleted: further suggest a

Formatted: Font colour: Text 2

Deleted: .

Deleted: However

Formatted: Font colour: Text 2

622 Kuznetsova and Lee, 2002; Kuznetsova *et al.*, 2004 and Reinthaler *et al.*, 2008). Carlson (1983) suggests that the distribution
623 of some organic fractions between the SML and the ULW may be governed by specific partitioning processes. For instance,
624 while Chen *et al.* (2016) point out the significant role of the ULW in DOC and CHO accumulation in the SML, Dietz *et al.*
625 (1976) observe fairly consistent abundances for these compounds between the two layers. Our experiments also show strong
626 1:1 correlation for DOC (Fig. 6(c)) and CHO (Fig. 6(j)), suggesting an absence of preferential affinity towards the SML (unlike
627 surfactants), which further indicates that their enrichment is predominantly controlled by the ULW. Although CHO, AA and
628 FA are identified to be the key constituents of the organic carbon pool (Hedges *et al.*, 1994), our correlation results reveal that
629 their partitioning between the SML and the ULW and, their eventual enrichment patterns, may not be consistent (Figure 6). ~~as~~
630 ~~also suggessted by Fig. 8.~~

631 4.1.3 Influencing factors and current uncertainties

632 Baier *et al.* (1974), Hunter and Liss (1981) and MacIntyre (1974) argue that the compositional diversity of the SML prevents
633 single compounds from fully representing the dissolved OM class, which further emphasizes the importance of assessing
634 compound-specific accumulation in the SML. Such investigations could shed light on selective and non-selective enrichment
635 dynamics of OM. An analysis of EF-based PDFs for various AA fractions (Figure 9(a)) – Total AA (TAA), Dissolved Free
636 AA (DFAA), Dissolved Combined AA (DCAA) and Particulate AA (PAA) – revealed notable heterogeneity within this
637 compound class, reflecting the chemical diversity and complexity of OM enrichment in the SML: ~~Relatively lower enrichment~~
638 ~~in DFAA may indicate its limited accumulation in the SML, potentially due to its high solubility and rapid turnover (Jørgensen~~
639 ~~et al., 1993). In contrast, DCAA, which comprises combined amino acids, might exhibit stronger surface activity and a greater~~
640 ~~tendency to form aggregates, leading to higher enrichment across a broader range. The bimodal EF distribution observed for~~
641 ~~PAA could reflect differences in particle composition, size and hydrophobicity, whereby denser particles sink rapidly while~~
642 ~~buoyant, organic-rich particles preferentially accumulate at the surface. TAA, which integrates all these molecular states, may~~
643 ~~dampen these extremes and yields more moderate enrichment. These interpretations remain as hypotheses, as very little is~~
644 ~~known about the behavior of AA, embedded in highly complex structures in natural SML.~~

645 Additionally, consistent with previous studies that investigated the influence on environmental drivers on the enrichment
646 dynamics in the SML (e.g., Asher, 1997; Barthelmeß *et al.*, 2021; Knulst *et al.*, 1997; Kuznetsova *et al.*, 2004; Liu and Dickhut,
647 1998; Obernosterer *et al.*, 2008; Reinthaler *et al.*, 2008; Tsai and Liu, 2003), our analysis demonstrates that factors such as
648 sampling location (for DOC), sampling season (for CHO) and sampling method (for DOC) (Figs. 9(b) – (d)) play key roles in
649 modulating the enrichment variability of the OM. ~~It~~ should be noted that these specific target compounds are chosen as
650 representative examples because they span all subcategories of secondary data considered in the study (see Supplementary
651 Table S1), and therefore enable a more robust comparison among different settings.

Formatted: Font colour: Text 2

Deleted: .

Formatted: Font colour: Text 2

Formatted: Don't suppress line numbers, Tab stops: 6,25 cm, Left

Deleted: 8

Formatted: Font colour: Text 2

Formatted: Font: Italic, Font colour: Text 2

Formatted: Font colour: Text 2

Deleted: .

Formatted: Font: (Default) Times New Roman, 10 pt, Font colour: Text 2, English (US)

Formatted: Default Paragraph Font, Font: (Default) Times New Roman, 10 pt, Font colour: Text 2, English (US)

Formatted: Default Paragraph Font, Font: Font colour: Text 2, English (US)

Formatted: Font: (Default) Times New Roman, 10 pt, Font colour: Text 2, English (US)

Formatted: Font: (Default) Times New Roman, 10 pt, Font colour: Text 2, English (US)

Formatted: Suppress line numbers

Deleted: 8

Formatted: Font colour: Text 2

Deleted: (

Deleted: i

Deleted:)

Formatted: Suppress line numbers

659 Comparison of DOC enrichment across four sampling locations (Fig. 9(b)) reveals relatively reduced coastal enrichment (as
660 also seen by Carlson, 1983). This pattern may result from enhanced mixing and shorter surface residence times due to stronger
661 wave action, tidal influence, or nearshore turbulence. Alternatively, the limited two-dimensional space at the air-sea interface
662 in combination with a highly saturated underlying water layer could also contribute to reduced enrichment. At the same time,
663 broader EF variability displayed by oceanic sites likely stems from the greater heterogeneity of open-ocean conditions
664 including varying biological productivity and OM sources (Carlson, 1983). In contrast, estuarine and freshwater systems,
665 which often have more constrained physical regimes and relatively consistent OM inputs, tend to exhibit narrower EF ranges
666 (Hillbricht-Ilkowska and Kostrzewska-Szlakowska, 2004). Observations by Barthelmeß *et al.* (2021) and Mustafa *et al.*
667 (2018) suggest that changes in EFs in these systems are driven more by variations in the ULW than by the SML itself, consistent
668 with the idea that the surface layer in high-OM regimes is already saturated and thus less responsive to additional inputs.
669 Moreover, bimodal CDFs of TOC for the SML and ULW concentrations (Fig. 4(a)) along with the distinct separation of three
670 data clusters in their correlation patterns (Fig. 6(a)), further highlight the significant role of spatial factors in shaping SML
671 composition. The origins of TOC data used in this study illustrates this variability: Data from (1) a heavily polluted urban lake
672 (concentration range: 12 – 16 mg L⁻¹; Baastrup-Spohr and Staehr, 2009), (2) a forested lake (concentration range: 3 – 5 mg L⁻¹;
673 Baastrup-Spohr and Staehr, 2009), (3) the Arctic Ocean (concentration range: 1 – 3 mg L⁻¹; Gao *et al.*, 2012) and (4) an
674 upwelling filament (concentration range: 3 – 4 mg L⁻¹; Barthelmeß *et al.*, 2021).

675 Seasonal comparison of the EF values for CHO (Fig. 9(c)) likely reflects temporal differences in biological drivers (Gašparović
676 and Čosović, 2001; 2003) in the SML (i.e., depletion in winter, while the other seasons show relatively higher and consistent
677 enrichment with broader variability). Additionally, stronger wind conditions typical of winter may disturb the SML and reduce
678 particle residence time, counteracting surface accumulation (Sun *et al.*, 2018). However, the influence on wind speed on SML
679 enrichment remains ambiguous; our comparison of EF values under calm (< 6.6 ms⁻¹; Reinthaler *et al.*, 2008) and rough (> 6.6
680 ms⁻¹) wind conditions yield inconclusive results (Supplementary Figure S2) with wind speed appearing to have little/no effect
681 on the SML enrichment (e.g., Baastrup-Spohr and Staehr, 2009 and Sabbaghzadeh *et al.*, 2017) or with enrichment persisting
682 even under rough sea conditions (e.g., Kuznetsova *et al.*, 2004; Reinthaler *et al.*, 2008), opposing the general understanding
683 that turbulent conditions may reduce the concentration in the SML (e.g., Carlson, 1983).

684 Nevertheless, it is important to note that imbalanced sampling efforts among these categories, (Supplementary Figure S1),
685 specially with regards to wind speed (Supplementary Figure S2; see the sample sizes), may compromise the robustness and
686 validity of these findings. This is also evident in the comparison of sampling techniques for the EF values of DOC (Fig. 9(d)),
687 where the drum method, with a sample size of only 17, shows limited variability compared to the screen and plate methods
688 (sample sizes of 80 and 110, respectively). This likely reflects a bias due to sampling effort rather than a true difference in
689 enrichment behavior. Collectively, these findings highlight the need for future SML research and SML-based model

Formatted [37]

Deleted: (...arlson, , [38]

Formatted [39]

Deleted: (

Deleted: ,

Deleted: ;

Formatted: Font: Italic, Font colour: Text 2

Formatted: Font colour: Text 2

Formatted: Font: Italic, Font colour: Text 2

Deleted: .

Deleted:)

Formatted: Font colour: Text 2

Formatted [40]

Moved (insertion) [3]

Formatted: Font colour: Text 1

Deleted: external environmental

Formatted [41]

Formatted: Suppress line numbers

Formatted [42]

Deleted: Gašparović and Čosović,

Formatted [43]

Moved (insertion) [2]

Deleted: T

Formatted [44]

Formatted: Suppress line numbers

Formatted [45]

Moved up [3]: Moreover, bimodal CDFs of TOC for the SML and ULW concentrations (Fig. 4(a)) along with the distinct separation of three data clusters in their correlation patterns (Fig. 6(a)), further highlight the significant role of external environmental factors in shaping SML composition. The origins of TOC data used in this study illustrates this variability: Data from (1) a heavily polluted urban lake (concentration range: 12 – 16 mg L⁻¹; Baastrup-Spohr and Staehr, 2009), (2) a forested lake (concentration range: 3 – 5 mg L⁻¹; Baastrup-Spohr and Staehr, 2009), (3) the Arctic Ocean (concentration range: 1 – 3 mg L⁻¹; Gao *et al.*, 2012) and (4) an upwelling filament (concentration range: 3 – 4 mg L⁻¹; Barthelmeß *et al.*, 2021). ¶

Moved up [2]: The influence on wind speed on SML enrichment remains ambiguous; our comparison of EF values under calm (< 6.6

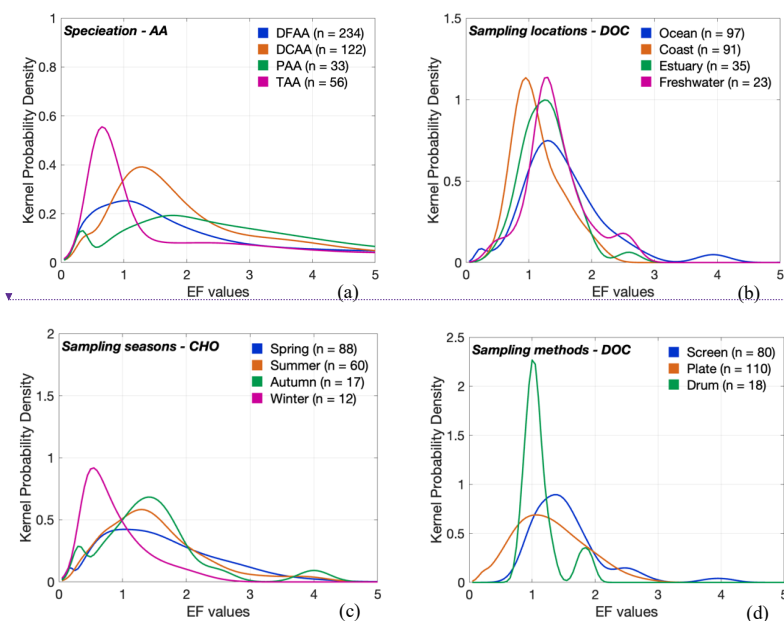
Deleted: ¶

Formatted [46]

Formatted [47]

Formatted [48]

763 [development to systematically account for wind and sea-state conditions, and to explore how enrichment patterns may vary](#)
764 [under different environmental regimes and methodological settings.](#)



765 **Figure 9: Factor-specific enrichment variability in the SML.** PDFs illustrating varying enrichment patterns for (a) AA across chemical
766 forms, (b) DOC across sampling locations, (c) CHO across sampling seasons and (d) DOC across sampling methods. 'n' gives the sample
767 size of each category. Supplementary Table S1 summarizes different sampling locations, sampling seasons and sampling methods observed
768 for the investigated target compounds.

769 [Another major source of uncertainty arises from the variability in sampling depths of the ULW \(Supplementary Table S1\),](#)
770 [which can affect the comparability of different data across multiple studies that would eventually introduce bias into the](#)
771 [interpretation of overarching trends. Additional biases which are beyond the scope of this study include the potential influence](#)
772 [of diurnal cycles \(López-Puertas et al., 2025\); OM can be rapidly removed from the SML through photochemical degradation](#)
773 [\(Obernosterer et al., 2008\) and also be affected by reduced bacterial metabolism due to solar radiation \(Dietz et al., 1976\).](#)
774 [Therefore, taken together, our meta-data analysis suggests that, investigating SML enrichment without accounting for these](#)

Formatted: Font colour: Text 2

Formatted: Suppress line numbers

Deleted: ¶

Deleted: 8

Formatted: Font colour: Text 2

Formatted: Normal, Suppress line numbers

Moved (insertion) [4]

Formatted: Font: 10 pt, Not Bold, Font colour: Text 2

Formatted: Caption, Line spacing: 1,5 lines, Don't suppress line numbers

777 influencing factors may mask true enrichment patterns, limiting the ability to derive meaningful insights. In light of these
778 considerations, our work highlights the need for conducting species-specific and condition-dependent analyses in future SML
779 research that also focus on subsequent environmental parameters, as also proposed by Pereira et al. (2018).

780 **4.2 Scale-related biases in EF estimates**

781 Accurate data interpretation is essential to gain precise insights and arrive at substantiated conclusions (Isles, 2020; Menge *et*
782 *al.*, 2018). This is particularly true for meta-analyses involving continuous environmental data where values may vary by
783 several orders of magnitude (e.g., Vitousek, 2004). In our study, when the PDF_C vs. PDF_N (Fig. 1) and PDF_D vs. PDF_P (Fig.
784 2) are evaluated on a linear scale (panels (a)), they exhibit right-skewness, whereas their log-transformed versions approximate
785 normal distributions (panels (b)). Comparisons between highly skewed distributions raise uncertainties as their offsets are
786 often dominated by extreme values/outliers. In contrast, when log transformation is applied, the distributions tend to exhibit
787 more symmetric, normalized patterns which enable direct comparisons in shape and spread across different categories (Zuur
788 *et al.*, 2007). Therefore the normality assumption for EF is inappropriate and the computation of an arithmetic mean, a
789 conventional practice adopted in many earlier works (e.g., Gašparović *et al.*, 2007; Gao *et al.*, 2012; Kuznetsova *et al.*, 2005;
790 Williams *et al.*, 1986; Wurl and Homes, 2008; Wurl *et al.*, 2009), can be misleading, likely providing a biased general picture
791 of OM enrichment in the SML.

792 The here constructed PDFs given in Figures 1 and 2 reveal that both mode (x_m ; shown by solid straight lines) and arithmetic
793 mean (x_a ; shown by dashed straight lines) differ between the two scales: The mode reflects the peak of a distribution and is
794 sensitive to the shape of its respective density curve. It varies depending on whether a dataset is in 'skewed' linear space or
795 'normalized' log space and becomes ambiguous in polymodal distributions (regardless of the scale: e.g. Fig. 3). As a
796 consequence, the mode in general provides an unreliable measure of central tendency. While the linear-arithmetic mean, which
797 is influenced by outliers, result in biases that exaggerate the corresponding central tendency, the log-arithmetic mean prevents
798 the extreme values from being dominant through balanced averaging and hence provides a reliable estimation of central
799 tendency. Nevertheless, geometric mean in linear space (x_g ; straight lines with alternating dots and dashes) is a meaningful
800 measure given that it is equivalent to the exponential of the arithmetic mean in logarithmic space (See Eqs. (B1) and (B2)).
801 Median (x ; dotted straight lines), on the other hand, remains relatively consistent across both scales as it is a rank-based
802 measure of central tendency that is unaffected by the magnitude of outliers. Accordingly, we suggest that future SML
803 enrichment studies employ a logarithmic scale for data analyses, and adopt either geometric mean and/or median on linear
804 scale or arithmetic mean and/or median on logarithmic scale for reliable trend analysis.

805 Based on these new insights on scale transformations and central tendency metric considerations, we have redefined the typical
806 EF values of the studied target compounds and their degrees of spread from a meta-analytical perspective, from the estimated
807 x , x_a and thresholds (i.e. UT and LT) of their PDFs (Fig. 3). To re-establish these EF ranges as generally observed estimates

Deleted: ¶

Moved up [4]: Another major source of uncertainty arises from the variability in sampling depths of the ULW (Supplementary Table S1), which can affect the comparability of different data across multiple studies that would eventually introduce bias into the interpretation of overarching trends. Additional biases which are beyond the scope of this study include the potential influence of diurnal cycles (López-Puertas *et al.*, 2025); OM can be rapidly removed from the SML through photochemical degradation (Obenosterer *et al.*, 2008) and also be affected by reduced bacterial metabolism due to solar radiation (Dietz *et al.*, 1976). Therefore, taken together, our meta-data analysis suggests that, investigating SML enrichment without accounting for these influencing factors may mask true enrichment patterns, limiting the ability to derive meaningful insights. In light of these considerations, our work highlights the need for conducting species-specific and condition-dependent analyses in future SML research that also focus on subsequent environmental parameters, as also proposed by Pereira *et al.* (2018).¶

827 under common conditions, ‘the box plot method’ (Tukey, 1977) was applied to the data to detect and remove potentially
828 extreme EF values that rarely occur in nature. By providing these systematically derived ranges, our analysis offers a robust
829 and comprehensive reference framework, enabling future SML-based studies to consistently evaluate newly obtained EF
830 measurements, assess their position relative to typical distributions, and identify deviations that may indicate unusual
831 environmental conditions or methodological inconsistencies.▼

Deleted: introduced by

Formatted: Font colour: Text 2

832 4.3 Role of EF in reflecting SML enrichment

833 While the metric of EF offers a convenient way to assess the accumulation trends in the SML and therefore serves as the basis
834 for many established insights and inferences in existing SML research (see Introduction), its ability to accurately and robustly
835 express the ‘true’ enrichment nature of the SML has constantly been a question of interest (e.g., Basstrup-Spohr and Staehr,
836 2009; Hillbricht-Ilkowska & Kostrzevska-Szlakowska, 2004; Knulst *et al.*, 1997; Kuznetsova *et al.*, 2004; Liss and Duce,
837 1997; Münster *et al.*, 1998; Södergren, 1987). The EF is a ratio that expresses the ‘relative’ changes in $[C]_{\text{SML}}$ with respect to
838 $[C]_{\text{ULW}}$ (Eq. (1)), and hence is sensitive to the variations in either layer. Ideally, to effectively reflect conditions of growing
839 SML enrichment, EF values should gradually rise in response to increasing $[C]_{\text{SML}}$ and decreasing $[C]_{\text{ULW}}$, which can be visibly
840 observed for DON (Fig. 7(f)), AA (Fig. 7(g)) and CHO (Fig. 7(j)). Nevertheless, our meta-analysis highlights several
841 inconsistencies that challenge the relevance of the EF values as indicators of ‘true’ SML enrichment. For instance, on one
842 hand, similar EF values can be observed for both oligotrophic and eutrophic environments (referring to the EFs of TOC: Fig.
843 7(a)), which limits the ability to distinguish the differences in their trophic status i.e., nutrient/productivity characteristic of
844 the water body, despite them being conspicuous in TOC’s absolute concentration range (bimodal CDFs; Fig. 4(a)). On the
845 other hand, high (low) EF values may occur under oligotrophic (eutrophic) conditions leading to over- (under-) estimation of
846 ecological setting i.e., biological and environmental context under which SML samples were collected; Fig. 7(g)).
847 Furthermore, symmetrical changes in SML and ULW yield near-constant EF values across a wide range of concentrations
848 (Fig. 7(c)), which could cause misinterpretations in key ecosystem shifts. We have also observed consistent EF values, even
849 when SML and ULW concentrations vary over several orders of magnitudes (Figs. 6(g) – (j)), which further raise concerns
850 over the metric’s robustness. Therefore, although widely used, EF values should be interpreted with caution and, combined
851 with additional parameters that provide more accurate information about the true enrichment behaviour of the SML.

Deleted: This method considers the values at 25th and 75th percentiles (also known as ‘Q₁’ and ‘Q₃’, respectively) of each distribution and computes a statistical estimate – Interquartile Range (also known as ‘IQR’) – by the difference between Q₃ and Q₁ (i.e., $IQR = Q_3 - Q_1$). If a datapoint falls outside the range of $Q_3 + IQR \times 1.5$ (also known as ‘upper bound’) and $Q_1 - IQR \times 1.5$ (also known as ‘lower bound’), it is considered atypical and therefore excluded from the analysis. This outlier detection approach is widely used across a broad range of research (e.g., Barbato *et al.*, 2011; Carling, 2000; Hoaglin *et al.*, 1986).

Deleted: the

Formatted: Font colour: Text 2

Formatted: Font colour: Text 2

852 A complementary parameter would be the typical upper limit of a $[C]_{\text{SML}}$ distribution which may reflect the maximum
853 concentration capacity of the SML. Such a measure can serve as a robust concentration estimate of such maximum capacity if
854 approximated from a meta-data derived distribution that includes observations across all diverse environmental conditions.
855 Table 1 summarizes the upper $[C]_{\text{SML}}$ threshold estimates (i.e., UT; at 95th percentile) for the target compounds, based on their
856 CDFs (Fig. 4). Although the robustness of these values largely depends on the quality and the scope of the underlying metadata,
857 our bootstrapping approach addresses these potential limitations. Nevertheless, we acknowledge that these estimates remain
858 data-constrained and therefore can improve with the inclusion of more comprehensive, high-resolution datasets across diverse

871 environmental conditions. Measured concentrations beyond these thresholds must be considered exceptionally high and
 872 warrant closer investigation to determine whether they reflect specific compounds or environmental conditions, such as
 873 biogeochemical, oceanographic and weather-related factors. High concentrations of CHO ($> 50 \mu\text{mol L}^{-1}$) were reported by
 874 Milinković et al. (2022), which affect the outcome of the UT estimate. In contrast, typical CHO concentrations in the SML
 875 reported in other studies remain well below the $50 \mu\text{mol L}^{-1}$. Since these differences cannot be resolved here, our UT estimate
 876 for CHO should therefore be treated with caution. ▲ ▲

877 **Table 1: A summary of estimated UT values (upper threshold; concentration at 95th percentile) for [C]_{SML} distributions of the target**
 878 **compounds.** This metric represents the maximum accumulation capacity of a certain compound in the SML. The values are rounded to the
 879 nearest whole number.

| Compound | TOC mg L ⁻¹ | POC mg L ⁻¹ | DOC mg L ⁻¹ | TON mg L ⁻¹ | PON mg L ⁻¹ | DON mg L ⁻¹ | AA $\mu\text{mol L}^{-1}$ | FA $\mu\text{g L}^{-1}$ | TEP $\mu\text{g Xeq L}^{-1}$ | CHO $\mu\text{mol L}^{-1}$ | Lipids $\mu\text{mol L}^{-1}$ | Proteins $\mu\text{mol L}^{-1}$ |
|----------|---------------------------|---------------------------|---------------------------|---------------------------|---------------------------|---------------------------|------------------------------|----------------------------|---------------------------------|-------------------------------|----------------------------------|------------------------------------|
| UT value | 14.0 | 11.0 | 10.0 | 2.0 | 1.0 | 0.5 | 6.0 | 46.0 | 6166.0 | 56.0 | 8.0 | 30.0 |

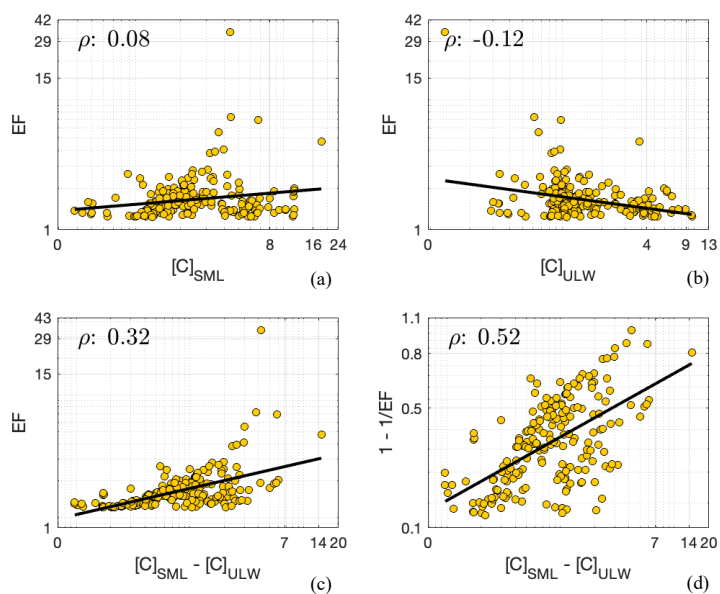
880 Considering absolute changes in the SML concentrations (rather than relative changes) – calculated as the magnitude difference
 881 between corresponding SML and ULW concentrations (i.e., $[C]_{\text{SML}} - [C]_{\text{ULW}}$) – provides complementary insights into the
 882 SML's enrichment dynamics. When this metric is compared against the EF values for DOC data where $\text{EF} > x$ ($= 1.2$), resulting
 883 Spearman's correlation coefficients (ρ) reveal a stronger relationship (Figure 10(c); $\rho = 0.32$) relative to EF vs. $[C]_{\text{SML}}$ (Figure
 884 10(a); $\rho = 0.08$) and EF vs. $[C]_{\text{ULW}}$ (Figure 10(b); $\rho = -0.12$) correlations. This implies that although the EFs may have a limited
 885 capacity to represent the absolute concentrations of either SML or ULW, they are more responsive to the absolute concentration
 886 'changes' in the two compartments. This analysis reveals that although 'enrichment factor' obscures accurately interpreting
 887 the trophic status or the actual enrichment in the SML, it may still hold value as a proxy that reflects the degree of partitioning
 888 between the surface microlayer and underlying waters.

889 Furthermore, normalization of $[C]_{\text{SML}} - [C]_{\text{ULW}}$ metric to the corresponding $[C]_{\text{SML}}$ values (i.e., $([C]_{\text{SML}} - [C]_{\text{ULW}}) / [C]_{\text{SML}}$)
 890 ultimately yields an EF-based metric: $1 - \frac{1}{\text{EF}}$. This expresses how much of the SML concentration is above the ULW baseline,
 891 effectively providing a measure of fractional enrichment that overlooks background variability in the ULW. Unlike
 892 conventional EF values, $1 - \frac{1}{\text{EF}}$ only ranges between 0 and 1. It rescales compound-specific variability in EF and is therefore
 893 better suited for comparison across all the different observational types; normalization of EF onto a common scale allows
 894 direct evaluations without bias from different units, magnitudes or concentration ranges. This metric better captures true trends,
 895 rather than artifacts/effects of scale, while enhancing visualization and communication of results. In addition, when compared
 896 against the absolute changes, this metric exhibits stronger correlation ($\rho = 0.52$; Fig. 10(d)), likely due to increased robustness
 897 to concentration variability obtained through its scale-dependent nature. As a result, when incorporated into modelling efforts,

- Deleted: within the SML
- Deleted: regarded as
- Formatted: Font colour: Text 2
- Deleted: should therefore find special attention
- Deleted: in particular with regard to the associated
- Deleted: conditions
- Formatted: Font colour: Text 2
- Formatted: Font colour: Blue
- Formatted: Font colour: Text 2

- Deleted: 9
- Deleted:
- Formatted: Font colour: Text 2
- Deleted: 9
- Deleted:
- Deleted: 9
- Deleted: c
- Deleted:
- Formatted: Font colour: Text 2
- Formatted: Font colour: Text 2
- Formatted: Font colour: Text 1
- Formatted: Font colour: Text 2
- Deleted: n
- Deleted:
- Formatted: Font colour: Text 2
- Formatted: Font colour: Text 2
- Deleted: 9
- Formatted: Font colour: Text 2

913 the normalized EF metric can offer distinct advantages such as integration of heterogenous datasets, consistent
 914 parameterization, easier comparisons of model predictions and robust sensitivity analyses. Together, these benefits contribute
 915 to more reliable and generalizable models of SML processes.



916 **Figure 10:** Correlations between EF and (a) $[C]_{SML}$, (b) $[C]_{ULW}$, (c) $[C]_{SML} - [C]_{ULW}$ and, (d) correlation between $1 - 1/EF$ and $[C]_{SML} - [C]_{ULW}$. These plots were generated for DOC data, in order to investigate the observed lack of correlation among EF – $[C]_{SML} - [C]_{ULW}$,
 917 as shown by Fig. 7(c).
 918

Deleted: 9

Formatted: Font colour: Text 2

919 5. Conclusion

920 [This study presents the first known meta-analysis of the SML, integrating a broad dataset of \$\[C\]_{SML}\$ and \$\[C\]_{ULW}\$ measurements](#)
 921 [to resolve methodological inconsistencies and establish a consensus-based understanding of SML enrichment dynamics. By](#)
 922 [meeting the statistical requirements for combining EF data and applying KDE as a robust analytical framework, we provide](#)
 923 [reliable distributional estimates and redefine typical EF ranges for 12 organic compounds, offering a comprehensive reference](#)
 924 [for assessing whether new observations fall within expected conditions or reflect unusual enrichment. Our results indicate that](#)
 925 [nitrogen-rich compounds and particulate OM exhibit stronger enrichment than carbon-rich and dissolved compounds.](#)

927 Nevertheless, the differing enrichment behavior of individual surfactants highlights that their surface-active properties, rather
928 than elemental composition alone, govern overall SML enrichment. Amongst these, the fatty acids clearly show the greatest
929 potential for high enrichment in the SML. This emphasizes the need to consider compound-specific chemistry as well as
930 environmental and methodological variability when interpreting SML processes, assessing their role in global gas flux
931 estimates and, developing models. Our assessment also inquired into the suitability of EF values as indicators of true SML
932 enrichment and suggests that, while EFs capture relative partitioning between the SML and ULW, they fall short in resolving
933 trophic variability. This study proposes complementary metrics (i.e., absolute concentration differences, SML concentration
934 capacities and fractional enrichment) that isolate true SML enrichment and support improved SML modelling. Finally, we
935 demonstrate that logarithmic transformations and robust central tendency metrics substantially improve statistical reliability
936 and data comparability over traditional linear-scale approaches, providing essential methodological guidance for future SML
937 research and its application to global air-sea exchange studies.

938 Appendix A: KDE method – additional information

939 Although the most basic non-parametric method to derive a probability distribution is histograms, they present two key
940 limitations for comparative studies: (1) unequal sample sizes across comparative groups restrict the use of uniform binning
941 and, (2) imposing uniform bin sizes potentially mask important distributional characteristics. In contrast, KDE circumvents
942 these issues by accounting a datapoint's exact value rather than assigning it to a particular bin of a certain width. This describes
943 the true underlying distribution of the data and allows more consistent and detailed comparisons of distributions. In this
944 analysis, we use Gaussian kernels – smooth, bell-shaped functions based on normal distribution – that weight observations
945 based on their distance. Chen (2017) and the references therein provide a comprehensive review of the KDE and its recent
946 advances.

947 In Gaussian kernels, bandwidth is analogous to standard deviation. In this study, the bandwidths for the linear KDEs were
948 computed based on an approach that includes a bias-variance trade-off. Briefly, the bias-variance trade-off represents kernels
949 that have a bandwidth that avoids too much variance in the estimates (i.e., bandwidths are not too small) while it does not
950 introduce too much bias for ranges that actually exhibit no data points (i.e., bandwidths are not too large). Calculations of
951 optimal bandwidth applied herein and an example of a bias-variance trade-off are described in Schartau *et al.*, (2010).
952 Nevertheless, in log-space, unlike in linear-space, data are more evenly distributed and hence fixed bandwidths avoid over-
953 smoothing of low values and under-smoothing of high values.

954 The selection of an optimal bandwidth for KDEs is influenced by sample size; smaller sample sizes lead to sparse and noisy
955 distributions which require more smoothing and therefore larger bandwidths. Excessively large bandwidths can result in
956 underfitting. In contrast, larger sample sizes may allow excessively smaller bandwidths that can lead to overfitting. Bootstrap

Deleted: not

Deleted: The here presented extensive data collection of $[C]_{SML}$ and $[C]_{ULW}$ measurements of various observational types of organic matter compounds is unique. Although the physical and biogeochemical properties of the SML have been studied in detail across diverse disciplines of aquatic science, to our knowledge, this study is the first to adopt a meta-analytical approach to bridge between insights of individual findings documented in the literature. Our quantitative assessment on the distributional characteristics of 12 organic compounds in the SML yielded statistically robust results owing to the use of the KDE method as the primary analytical technique, which enabled a coherent comparison of multivariate data.

Our results indicate that nitrogen-rich compounds and particulate OM tend to be more enriched in the SML compared to carbon-rich compounds and dissolved OM. These findings underscore the need for future SML research to focus on the species-specific chemistry of OM, specifically surfactants, along with the variability of external influencing factors, in order to better understand and approximate their role in global gas flux estimates. Informed by this, we explore EF values by re-evaluating the typical ranges, previously defined in individual studies, through a meta-analytical perspective. Our assessment also inquired into the suitability of EF values as indicators of true SML enrichment and suggests that, while the EF, which expresses relative changes in the SML compared to the ULW, can reflect the partition variability between the two layers, it falls short in capturing trophic variability.

Deleted: . The latter plays a crucial role in determining ecosystem structure. In light of the foregoing, we propose that EF estimates be complemented with additional parameters such as the absolute concentration differences between the SML and the ULW and the maximum concentration capacities within the SML, to provide a more in-depth understanding of enrichment dynamics.

Deleted: In addition to the primary outcomes, a noteworthy secondary insight from this study is the importance of selecting an appropriate data transformation scale (i.e. linear or logarithmic) and a robust measure of central tendency (i.e. mode, median, arithmetic mean or geometric mean) to ensure accurate data representation and reliable inference in future SML research. Our analysis provides strong evidence for the following advantages of transforming data into logarithmic scale: (1) it facilitates meaningful ratio comparisons such as the EF by converting multiplicative relationships into additive ones; (2) it better reflects the log-normality characteristics of the dependencies between $[C]_{SML}$ and $[C]_{ULW}$, which improves statistical model performance; (3) it was shown to promote homoscedasticity and (4) it enhances robustness, accuracy and interpretability of central tendency metrics.

1002 resampling addresses these potential uncertainties in our analysis and, ensures the robustness and precision of the estimated
1003 density distributions. Deviations between the bootstrapped KDEs and their ensemble mean were found to approximate a
1004 normal distribution (consistent with Central Limit Theorem). Therefore, these ensemble means can be regarded as reliable
1005 representations of the underlying data, supporting valid comparisons of probability distributions across different groups or
1006 clusters.

1007 Appendix B: Mathematical expressions of distributional characteristics

1008 If a dataset contains values of ' x_i ' with a sample size of ' n ', mode (x_m) is the most frequently occurring value in the dataset
1009 and therefore, the point where a PDF reaches its highest density. A distribution appears to be the most concentrated at x_m .
1010 Median (x) returns the value at the 50th percentile of an ascending dataset. It divides the area under a PDF into two equal
1011 halves. The arithmetic mean (x_a), is the average of a distribution, given by the following equation:

$$1012 \sum_{i=1}^n \frac{x_i}{n} \quad (B1)$$

1013 x_a gives the point where weighted sum of a PDF is balanced. However, in the case of datasets that range over several orders
1014 of magnitudes, the geometric mean (hereafter referred to as ' x_g ') is the more preferred central tendency estimate, as it accounts
1015 for the relative proportions of values (as opposed to their absolute magnitudes as is the case in x_a) and hence, is less sensitive
1016 to outliers. x_g is calculated by the following equation:

$$1017 \left(\prod_{i=1}^n x_i \right)^{\frac{1}{n}} \quad (B2)$$

1018 x_g of a linear distribution is mathematically equal to the exponentiated x_a of the log-transformed version of the same
1019 distribution.

1020 In addition, the following equation, which accounts for the squared differences across all the datapoints of the corresponding
1021 CDFs, estimates the discrete form of the integrated quadratic distance (IQD, explained in section 2.2.2), with $\Delta x_i = x_i - x_{i-1}$:

$$1022 IQD = \sum_{i=1}^n \left(\left(CDF_{C_{SML}(x_i)} - CDF_{C_{ULW}(x_i)} \right)^2 \times \Delta x_i \right) \quad (B3)$$

1023 A higher IQD value implies that the divergence is greater and therefore the corresponding CDFs are more different.

1024 Code availability

1025 [Computational codes used in this study are available at OceanRep GEOMAR | https://oceanrep.geomar.de/id/eprint/63615/](https://oceanrep.geomar.de/id/eprint/63615/)
1026 [↓](#) The repository includes the full implementation of the KDE method, representative example scripts demonstrating its
1027 application for generating probability density functions and cumulative density functions, and a script to reproduce the
1028 correlation plots presented in the manuscript.

Deleted: The computational codes used in this study are available upon request to A.S.

Formatted: Font colour: Text 2

Formatted: Font: (Default) Times New Roman, 10 pt, Font colour: Text 2, English (US)

Formatted: Space Before: 6 pt, After: 6 pt

Deleted: [repository name], [DOI or URL]

Formatted: Font: (Default) Times New Roman, 10 pt, Font colour: Text 2, English (US)

Formatted: Font: Font colour: Text 2, English (US)

1032 **Data availability**

1033 All data used in this study were extracted from previously published peer-reviewed sources [and are publicly available through](#)
1034 [the PANGAEA data repository \[https://doi.pangaea.de/10.1594/PANGAEA.990017 \]](#). Full citations for all the datasets are
1035 provided in supplementary information. No new data were generated for this study.

Formatted: Font colour: Text 2

Deleted: [DOI]

Formatted: Font colour: Text 2

1036 **Author contribution**

1037 A. S. – Data Curation, Conceptualization, Methodology, Formal Analysis, Visualization, Writing – Original Draft, Writing –
1038 Review & Editing
1039 S. N. – Data Curation, Writing – Review & Editing
1040 T. B. – Data Provision, Writing – Review & Editing
1041 A. E. – Funding Acquisition, Data Provision, Writing – Review & Editing
1042 H. H. – Data Provision, Writing – Review & Editing
1043 M. P. – Data Provision, Writing – Review & Editing
1044 K. W. – Methodology, Writing – Review & Editing
1045 O. W. – Funding Acquisition, Data Provision, Writing – Review & Editing
1046 M. S. – Conceptualization, Methodology, Formal Analysis, Visualization, Funding Acquisition, Supervision, Writing –
1047 Review & Editing

Deleted: ¶

1048 **Competing interests**

1049 Authors A. S., T. B., A. E. and M. S. are affiliated with the same institution as H. B., who serves as an overseeing editor for
1050 the special issue “*Biogeochemical processes and air-sea exchange in the sea-surface microlayer*”. Authors A. S., T. B., A.
1051 E., H. H., M. P., O. W. and M. S. are collaborators with H. B. on an ongoing research project. These potential competing
1052 interests have been fully disclosed to the journal. The authors declare no other competing interests relevant to the submitted
1053 work.

1054 **Acknowledgements**

1055 The authors gratefully acknowledge the support and collaboration of colleagues and institutions involved in this work. We also
1056 acknowledge the valuable contributions of the authors of previously published datasets that were used in this study. Their work
1057 provided essential input for our analysis. This study was conducted as part of the project “Biogeochemical processes and air-
1058 sea exchange in the sea-surface microlayer (BASS)”, and we thank all project partners for their support and scientific exchange.

1061 Data compilation had been initiated through the large integrated project Surface Ocean Processes in the Anthropocene
1062 (SOPRAN, 03F0662A), funded by the German Federal Ministry of Education and Research (BMBF).

1063 Financial support

1064 This work is supported by the project “Biogeochemical processes and air-sea exchange in the sea-surface microlayer (BASS)”,
1065 which is funded by the German Research Foundation (DFG) under Grant No 451574234: [SCHA 2123/1-1](#).

1066 References

- 1067 Allredge, A.L., Passow, U., Logan, B.E., 1993. The abundance and significance of a class of large, transparent organic
1068 particles in the ocean. *Deep Sea Res. Part Oceanogr. Res. Pap.* 40, 1131–1140. [https://doi.org/10.1016/0967-0637\(93\)90129-Q](https://doi.org/10.1016/0967-0637(93)90129-Q)
- 1070 Asher, W., 1997. The sea-surface microlayer and its effect on global air-sea gas transfer. *Sea Surf. Glob. Change* 251–286.
- 1071 Asmussen-Schäfer, F., Ribas-Ribas, M., Wurl, O., Friedrichs, G., 2026. Linking surface coverage with surfactant activity to
1072 refine the role of surfactants for air-sea gas exchange. <https://doi.org/10.5194/egusphere-2025-5276>
- 1073 Astrahan, P., Herut, B., Paytan, A., Rahav, E., 2016. The Impact of Dry Atmospheric Deposition on the Sea-Surface Microlayer
1074 in the SE Mediterranean Sea: An Experimental Approach. *Front. Mar. Sci.* 3.
1075 <https://doi.org/10.3389/fmars.2016.00222>
- 1076 Baastrup-Spohr, L., Staehr, P.A., 2009. Surface microlayers on temperate lowland lakes. *Hydrobiologia* 625, 43–59.
1077 <https://doi.org/10.1007/s10750-008-9695-3>
- 1078 Baier, R., DW, G., Perlmutter, S., King, R., 1974. Dominant chemical composition of sea-surface films, natural slicks, and
1079 foams.
- 1080 Barthelmeß, T., Engel, A., 2022. How biogenic polymers control surfactant dynamics in the surface microlayer: insights from
1081 a coastal Baltic Sea study. *Biogeosciences* 19, 4965–4992. <https://doi.org/10.5194/bg-19-4965-2022>
- 1082 Barthelmeß, T., Schütte, F., Engel, A., 2021. Variability of the Sea Surface Microlayer Across a Filament’s Edge and Potential
1083 Influences on Gas Exchange. *Front. Mar. Sci.* 8, 718384. <https://doi.org/10.3389/fmars.2021.718384>
- 1084 Brinis, A., Méjanelle, L., Momzikoff, A., Gondry, G., Fillaux, J., Point, V., Saliot, A., 2004. Phospholipid ester-linked fatty
1085 acids composition of size-fractionated particles at the top ocean surface. *Org. Geochem.* 35, 1275–1287.
1086 <https://doi.org/10.1016/j.orggeochem.2004.04.009>
- 1087 Carlson, D.J., 1983. Dissolved organic materials in surface microlayers: Temporal and spatial variability and relation to sea
1088 state. *Limnol. Oceanogr.* 28, 415–431. <https://doi.org/10.4319/lo.1983.28.3.0415>
- 1089 Carlucci, A.F., Craven, D.B., Henrichs, S.M., 1985. Surface-film microheterotrophs: amino acid metabolism and solar
1090 radiation effects on their activities.
- 1091 Cen-Lin, H., Tzung-May, F., 2013. Air-Sea Exchange of Volatile Organic Compounds: A New Model with Microlayer Effects.
1092 *Atmospheric Ocean. Sci. Lett.* 6, 97–102. <https://doi.org/10.1080/16742834.2013.11447063>
- 1093 Chen, Y., Yang, G.-P., Xia, Q.-Y., Wu, G.-W., 2016. Enrichment and characterization of dissolved organic matter in the
1094 surface microlayer and subsurface water of the South Yellow Sea. *Mar. Chem.* 182, 1–13.
1095 <https://doi.org/10.1016/j.marchem.2016.04.001>
- 1096 Chen, Y.-C., 2017. A tutorial on kernel density estimation and recent advances. *Biostat. Epidemiol.* 1, 161–187.
- 1097 Čosović, B., Vojvodić, V., 1998. Voltammetric Analysis of Surface Active Substances in Natural Seawater. *Electroanalysis*
1098 10, 429–434. [https://doi.org/10.1002/\(SICI\)1521-4109\(199805\)10:6%253C429::AID-ELAN429%253E3.0.CO;2-7](https://doi.org/10.1002/(SICI)1521-4109(199805)10:6%253C429::AID-ELAN429%253E3.0.CO;2-7)
- 1099 Čosović, B., Vojvodić, V., 1989. Adsorption behaviour of the hydrophobic fraction of organic matter in natural waters. *Mar.*
1100 *Chem.* 28, 183–198. [https://doi.org/10.1016/0304-4203\(89\)90194-1](https://doi.org/10.1016/0304-4203(89)90194-1)
- 1101 Crocetti, E., 2016. Systematic Reviews With Meta-Analysis: Why, When, and How? *Emerg. Adulthood* 4, 3–18.
1102 <https://doi.org/10.1177/2167696815617076>

Formatted: German

Formatted: German

- 1103 Cunliffe, M., Engel, A., Frka, S., Gašparović, B., Guitart, C., Murrell, J.C., Salter, M., Stolle, C., Upstill-Goddard, R., Wurl,
1104 O., 2013. Sea surface microlayers: A unified physicochemical and biological perspective of the air–ocean interface.
1105 Prog. Oceanogr. 109, 104–116. <https://doi.org/10.1016/j.pocan.2012.08.004>
- 1106 Cunliffe, M., Murrell, J.C., 2009. The sea-surface microlayer is a gelatinous biofilm. ISME J. 3, 1001–1003.
1107 <https://doi.org/10.1038/ismej.2009.69>
- 1108 Cunliffe, M., Salter, M., Mann, P.J., Whiteley, A.S., Upstill-Goddard, R.C., Murrell, J.C., 2009. Dissolved organic carbon and
1109 bacterial populations in the gelatinous surface microlayer of a Norwegian fjord mesocosm. FEMS Microbiol. Lett.
1110 299, 248–254. <https://doi.org/10.1111/j.1574-6968.2009.01751.x>
- 1111 Dietz, A.S., Albright, L.J., Tuominen, T., 1976. Heterotrophic activities of bacterioneuston and bacterioplankton. Can. J.
1112 Microbiol. 22, 1699–1709. <https://doi.org/10.1139/m76-251>
- 1113 Dukhin, S.S., Kovalchuk, V.I., Gochev, G.G., Lotfi, M., Krzan, M., Malysa, K., Miller, R., 2015. Dynamics of Rear Stagnant
1114 Cap formation at the surface of spherical bubbles rising in surfactant solutions at large Reynolds numbers under
1115 conditions of small Marangoni number and slow sorption kinetics. Adv. Colloid Interface Sci. 222, 260–274.
1116 <https://doi.org/10.1016/j.cis.2014.10.002>
- 1117 Engel, A., Bange, H.W., Cunliffe, M., Burrows, S.M., Friedrichs, G., Galgani, L., Herrmann, H., Hertkorn, N., Johnson, M.,
1118 Liss, P.S., Quinn, P.K., Schartau, M., Soloviev, A., Stolle, C., Upstill-Goddard, R.C., Van Pinxteren, M., Zäncker,
1119 B., 2017. The Ocean’s Vital Skin: Toward an Integrated Understanding of the Sea Surface Microlayer. Front. Mar.
1120 Sci. 4, 165. <https://doi.org/10.3389/fmars.2017.00165>
- 1121 Engel, A., Galgani, L., 2016. The organic sea-surface microlayer in the upwelling region off the coast of Peru and potential
1122 implications for air–sea exchange processes. Biogeosciences 13, 989–1007. <https://doi.org/10.5194/bg-13-989-2016>
- 1123 Engel, A., Thoms, S., Riebesell, U., Rochelle-Newall, E., Zondervan, I., 2004. Polysaccharide aggregation as a potential sink
1124 of marine dissolved organic carbon. Nature 428, 929–932. <https://doi.org/10.1038/nature02453>
- 1125 Feenstra, S., 2006. Use of logarithmic-scale correlation plots to represent contaminant ratios for evaluation of subsurface
1126 environmental data. Environ. Forensics 7, 175–185.
- 1127 Frew, N.M., 1997. The role of organic films in air–sea gas exchange, in: Liss, P.S., Duce, R.A. (Eds.), The Sea Surface and
1128 Global Change. Cambridge University Press, Cambridge, pp. 121–172.
1129 <https://doi.org/10.1017/CBO9780511525025.006>
- 1130 Frew, N.M., Bock, E.J., Schimpf, U., Hara, T., Haußecker, H., Edson, J.B., McGillis, W.R., Nelson, R.K., McKenna, S.P., Uz,
1131 B.M., Jähne, B., 2004. Air-sea gas transfer: Its dependence on wind stress, small-scale roughness, and surface films.
1132 J. Geophys. Res. Oceans 109, 2003JC002131. <https://doi.org/10.1029/2003JC002131>
- 1133 Frka, S., Pogorzelski, S., Kozarac, Z., Čosović, B., 2012. Physicochemical Signatures of Natural Sea Films from Middle
1134 Adriatic Stations. J. Phys. Chem. A 116, 6552–6559. <https://doi.org/10.1021/jp212430a>
- 1135 Gao, Q., Leck, C., Rauschenberg, C., Matrai, P.A., 2012. On the chemical dynamics of extracellular polysaccharides in the
1136 high Arctic surface microlayer. Ocean Sci. 8, 401–418. <https://doi.org/10.5194/os-8-401-2012>
- 1137 Garabetian, F., Romano, J.-C., Paul, R., Sigoillot, J.-C., 1993. Organic matter composition and pollutant enrichment of sea
1138 surface microlayer inside and outside slicks. Mar. Environ. Res. 35, 323–339. [https://doi.org/10.1016/0141-1136\(93\)90100-E](https://doi.org/10.1016/0141-1136(93)90100-E)
- 1140 Gašparović, B., Čosović, B., 2003. Surface-active properties of organic matter in the North Adriatic Sea. Estuar. Coast. Shelf
1141 Sci. 58, 555–566. [https://doi.org/10.1016/S0272-7714\(03\)00133-1](https://doi.org/10.1016/S0272-7714(03)00133-1)
- 1142 Gašparović, B., Čosović, B., 2001. Distribution of surface-active substances in the northern Adriatic Sea. Mar. Chem. 75, 301–
1143 313. [https://doi.org/10.1016/S0304-4203\(01\)00044-5](https://doi.org/10.1016/S0304-4203(01)00044-5)
- 1144 Gašparović, B., Plavšić, M., Čosović, B., Saliot, A., 2007. Organic matter characterization in the sea surface microlayers in
1145 the subarctic Norwegian fjords region. Mar. Chem. 105, 1–14. <https://doi.org/10.1016/j.marchem.2006.12.010>
- 1146 Goldman, J.C., Dennett, M.R., Frew, N.M., 1988. Surfactant effects on air-sea gas exchange under turbulent conditions. Deep
1147 Sea Res. Part Oceanogr. Res. Pap. 35, 1953–1970. [https://doi.org/10.1016/0198-0149\(88\)90119-7](https://doi.org/10.1016/0198-0149(88)90119-7)
- 1148 Härdle, W., Müller, M., Sperlich, S., Werwatz, A., 2004. Nonparametric and semiparametric models. Springer Science &
1149 Business Media.
- 1150 Harvey, H.R., Tuttle, J.H., Bell, J.T., 1995. Kinetics of phytoplankton decay during simulated sedimentation: Changes in
1151 biochemical composition and microbial activity under oxic and anoxic conditions. Geochim. Cosmochim. Acta 59,
1152 3367–3377. [https://doi.org/10.1016/0016-7037\(95\)00217-N](https://doi.org/10.1016/0016-7037(95)00217-N)

Formatted: German

Formatted: German

Formatted: German

- 1153 Hedges, J.I., Cowie, G.L., Richey, J.E., Quay, P.D., Benner, R., Strom, M., Forsberg, B.R., 1994. Origins and processing of
1154 organic matter in the Amazon River as indicated by carbohydrates and amino acids. *Limnol. Oceanogr.* 39, 743–761.
1155 <https://doi.org/10.4319/lo.1994.39.4.0743>
- 1156 Henrichs, S.M., Williams, P.M., 1985. Dissolved and particulate amino acids and carbohydrates in the sea surface microlayer.
1157 *Mar. Chem.* 17, 141–163. [https://doi.org/10.1016/0304-4203\(85\)90070-2](https://doi.org/10.1016/0304-4203(85)90070-2)
- 1158 Hillbricht-Ilkowska, A., Kostrzewska-Szlakowska, I., 2004. Surface microlayer in lakes of different trophic status: nutrients
1159 concentration and accumulation. *Pol. J. Ecol.* 52, 461–478.
- 1160 Hunter, K.A., 1980. Processes affecting particulate trace metals in the sea surface microlayer. *Mar. Chem.* 9, 49–70.
1161 [https://doi.org/10.1016/0304-4203\(80\)90006-7](https://doi.org/10.1016/0304-4203(80)90006-7)
- 1162 Hunter, K.A., Liss, P.S., 1981. Chapter 9 Organic Sea Surface Films, in: Duursma, E.K., Dawson, R. (Eds.), Elsevier
1163 Oceanography Series. Elsevier, pp. 259–298. [https://doi.org/10.1016/S0422-9894\(08\)70331-3](https://doi.org/10.1016/S0422-9894(08)70331-3)
- 1164 Hunter, K.A., Liss, P.S., 1977. The input of organic material to the oceans: air–sea interactions and the organic chemical
1165 composition of the sea surface. *Mar. Chem.* 5, 361–379. [https://doi.org/10.1016/0304-4203\(77\)90029-9](https://doi.org/10.1016/0304-4203(77)90029-9)
- 1166 Jørgensen, N., Kroer, N., Coffin, R., Yang, X.-H., Lee, C., 1993. Dissolved free amino acids, combined amino acids, and DNA
1167 as sources of carbon and nitrogen to marine bacteria. *Mar. Ecol. Prog. Ser.* 98, 135–148.
1168 <https://doi.org/10.3354/meps098135>
- 1169 Joux, F., Agogue, H., Obernosterer, I., Dupuy, C., Reinthaler, T., Herndl, G., Lebaron, P., 2006. Microbial community structure
1170 in the sea surface microlayer at two contrasting coastal sites in the northwestern Mediterranean Sea. *Aquat. Microb.*
1171 *Ecol.* 42, 91–104. <https://doi.org/10.3354/ame042091>
- 1172 Keene, O.N., 1995. The log transformation is special. *Stat. Med.* 14, 811–819. <https://doi.org/10.1002/sim.4780140810>
- 1173 Kjelleberg, S., Norkrans, B., Löfgren, H., Larsson, K., 1976. Surface balance study of the interaction between microorganisms
1174 and lipid monolayer at the air/water interface. *Appl. Environ. Microbiol.* 31, 609–611.
1175 <https://doi.org/10.1128/aem.31.4.609-611.1976>
- 1176 Knipping, E.M., Lakin, M.J., Foster, K.L., Jungwirth, P., Tobias, D.J., Gerber, R.B., Dabdub, D., Finlayson-Pitts, B.J., 2000.
1177 Experiments and Simulations of Ion-Enhanced Interfacial Chemistry on Aqueous NaCl Aerosols. *Science* 288, 301–
1178 306. <https://doi.org/10.1126/science.288.5464.301>
- 1179 Knulst, J.C., Backlund, P., Hessen, D.O., Riise, G., Södergren, A., 1997. Response of surface microlayers to artificial acid
1180 precipitation in a meso-humic lake in Norway. *Water Res.* 31, 2177–2186. [https://doi.org/10.1016/S0043-1354\(97\)00061-4](https://doi.org/10.1016/S0043-1354(97)00061-4)
- 1181
- 1182 Kock, A., Schafstall, J., Dengler, M., Brandt, P., Bange, H.W., 2012. Sea-to-air and diapycnal nitrous oxide fluxes in the
1183 eastern tropical North Atlantic Ocean. *Biogeosciences* 9, 957–964. <https://doi.org/10.5194/bg-9-957-2012>
- 1184 Kujawinski, E.B., Farrington, J.W., Moffett, J.W., 2002. Evidence for grazing-mediated production of dissolved surface-active
1185 material by marine protists. *Mar. Chem.* 77, 133–142. [https://doi.org/10.1016/S0304-4203\(01\)00082-2](https://doi.org/10.1016/S0304-4203(01)00082-2)
- 1186 Kurata, N., Vella, K., Hamilton, B., Shivji, M., Soloviev, A., Matt, S., Tartar, A., Perrie, W., 2016. Surfactant-associated
1187 bacteria in the near-surface layer of the ocean. *Sci. Rep.* 6, 19123. <https://doi.org/10.1038/srep19123>
- 1188 Kuznetsova, M., Lee, C., 2002. Dissolved free and combined amino acids in nearshore seawater, sea surface microlayers and
1189 foams: Influence of extracellular hydrolysis. *Aquat Sci* 64, 252–268.
- 1190 Kuznetsova, M., Lee, C., Aller, J., Frew, N., 2004. Enrichment of amino acids in the sea surface microlayer at coastal and open
1191 ocean sites in the North Atlantic Ocean. *Limnol. Oceanogr.* 49, 1605–1619.
1192 <https://doi.org/10.4319/lo.2004.49.5.1605>
- 1193 Laß, K., Bange, H.W., Friedrichs, G., 2013. Seasonal signatures in SFG vibrational spectra of the sea surface nanolayer at
1194 Boknis Eck Time Series Station (SW Baltic Sea). *Biogeosciences* 10, 5325–5334. <https://doi.org/10.5194/bg-10-5325-2013>
- 1195
- 1196 Laß, K., Friedrichs, G., 2011. Revealing structural properties of the marine nanolayer from vibrational sum frequency
1197 generation spectra. *J. Geophys. Res.* 116, C08042. <https://doi.org/10.1029/2010JC006609>
- 1198 Li, L., Wu, P., Zhang, P., Huang, S., Zhang, Y., 2024. An improved model for air–sea exchange of elemental mercury in
1199 MITgcm-ECCOv4-Hg: the role of surfactants and waves. *Geosci. Model Dev.* 17, 8683–8695.
1200 <https://doi.org/10.5194/gmd-17-8683-2024>
- 1201 Liss, P.S., Duce, R.A., 1997. The sea surface and global change. Cambridge University Press.

Formatted: German

Formatted: German

Formatted: German

Formatted: German

- 1202 Liu, K., Dickhut, R.M., 1998. Effects of wind speed and particulate matter source on surface microlayer characteristics and
1203 enrichment of organic matter in southern Chesapeake Bay. *J. Geophys. Res. Atmospheres* 103, 10571–10577.
1204 <https://doi.org/10.1029/97JD03736>
- 1205 López-Puertas, A., Wurl, O., Frka, S., Ribas-Ribas, M., 2025. Diel Variability Affects the Inorganic Marine Carbon System
1206 in the Sea-Surface Microlayer of a Mediterranean coastal area (Šibenik, Croatia). <https://doi.org/10.5194/egusphere-2025-2090>
- 1207
- 1208 MacIntyre, F., 1974. Chemical fractionation and sea-surface microlayer processes. *The sea* 5, 245–299.
- 1209 Maki, J.S., Hermansson, M., 2020. The dynamics of surface microlayers in aquatic environments. *Biol. Part. Aquat. Syst.*
1210 Second Ed. 161–182.
- 1211 Mari, X., Burd, A., 1998. Seasonal size spectra of transparent exopolymeric particles (TEP) in a coastal sea and comparison
1212 with those predicted using coagulation theory. *Mar. Ecol. Prog. Ser.* 163, 63–76. <https://doi.org/10.3354/meps163063>
- 1213 Mari, X., Passow, U., Migon, C., Burd, A.B., Legendre, L., 2017. Transparent exopolymer particles: Effects on carbon cycling
1214 in the ocean. *Prog. Oceanogr.* 151, 13–37. <https://doi.org/10.1016/j.pocan.2016.11.002>
- 1215 Marty, J.C., Saliot, A., 1976. Hydrocarbons (normal alkanes) in the surface microlayer of seawater. *Deep-Sea Res.* 23, 863–
1216 873.
- 1217 McKenna, S.P., McGillis, W.R., 2004. The role of free-surface turbulence and surfactants in air–water gas transfer. *Int. J. Heat*
1218 *Mass Transf.* 47, 539–553. <https://doi.org/10.1016/j.ijheatmasstransfer.2003.06.001>
- 1219 Menge, D.N.L., MacPherson, A.C., Bytnerowicz, T.A., Quebbeman, A.W., Schwartz, N.B., Taylor, B.N., Wolf, A.A., 2018.
1220 Logarithmic scales in ecological data presentation may cause misinterpretation. *Nat. Ecol. Evol.* 2, 1393–1402.
1221 <https://doi.org/10.1038/s41559-018-0610-7>
- 1222 Mengist, W., Soromessa, T., Legese, G., 2020. Method for conducting systematic literature review and meta-analysis for
1223 environmental science research. *MethodsX* 7, 100777. <https://doi.org/10.1016/j.mex.2019.100777>
- 1224 Milinković, A., Penezić, A., Kušan, A.C., Gluščić, V., Žužul, S., Skejić, S., Šantić, D., Godec, R., Pehcec, G., Omanović, D.,
1225 Engel, A., Frka, S., 2022. Variabilities of biochemical properties of the sea surface microlayer: Insights to the
1226 atmospheric deposition impacts. *Sci. Total Environ.* 838, 156440. <https://doi.org/10.1016/j.scitotenv.2022.156440>
- 1227 Mopper, K., Zhou, J., Sri Ramana, K., Passow, U., Dam, H.G., Drapeau, D.T., 1995. The role of surface-active carbohydrates
1228 in the flocculation of a diatom bloom in a mesocosm. *Deep Sea Res. Part II Top. Stud. Oceanogr.* 42, 47–73.
1229 [https://doi.org/10.1016/0967-0645\(95\)00004-A](https://doi.org/10.1016/0967-0645(95)00004-A)
- 1230 Münster, U., Heikkinen, E., Knulst, J., 1998. Nutrient composition, microbial biomass and activity at the air-water interface
1231 of small boreal forest lakes, in: Tamminen, T., Kuosa, H. (Eds.), *Eutrophication in Planktonic Ecosystems: Food Web*
1232 *Dynamics and Elemental Cycling*. Springer Netherlands, Dordrecht, pp. 261–270. https://doi.org/10.1007/978-94-017-1493-8_21
- 1233
- 1234 Mustafa, N.I.H., Badewien, T.H., Ribas-Ribas, M., Wurl, O., 2018. High-resolution observations on enrichment processes in
1235 the sea-surface microlayer. *Sci. Rep.* 8, 13122. <https://doi.org/10.1038/s41598-018-31465-8>
- 1236 Mustafa, N.I.H., Ribas-Ribas, M., Banko-Kubis, H.M., Wurl, O., 2020. Global reduction of *in situ* CO₂ transfer velocity by
1237 natural surfactants in the sea-surface microlayer. *Proc. R. Soc. Math. Phys. Eng. Sci.* 476, 20190763.
1238 <https://doi.org/10.1098/rspa.2019.0763>
- 1239 Myklestad, S.M., 1995. Release of extracellular products by phytoplankton with special emphasis on polysaccharides. *Sci.*
1240 *Total Environ.* 165, 155–164. [https://doi.org/10.1016/0048-9697\(95\)04549-G](https://doi.org/10.1016/0048-9697(95)04549-G)
- 1241 Obernosterer, I., Catala, P., Lami, R., Caparros, J., Ras, J., Bricaud, A., Dupuy, C., van Wambeke, F., Lebaron, P., 2008.
1242 Biochemical characteristics and bacterial community structure of the sea surface microlayer in the South Pacific
1243 Ocean.
- 1244 Obernosterer, I., Catala, P., Reinthaler, T., Herndl, G., Lebaron, P., 2005. Enhanced heterotrophic activity in the surface
1245 microlayer of the Mediterranean Sea. *Aquat. Microb. Ecol.* 39, 293–302. <https://doi.org/10.3354/ame039293>
- 1246 Parzen, E., 1962. On Estimation of a Probability Density Function and Mode. *Ann. Math. Stat.* 33, 1065–1076.
- 1247 Passow, U., 2000. Formation of transparent exopolymer particles, TEP, from dissolved precursor material. *Mar. Ecol. Prog.*
1248 *Ser.* 192, 1–11. <https://doi.org/10.3354/meps192001>
- 1249 Passow, U., Alldredge, A.L., 1999. Do transparent exopolymer particles (TEP) inhibit grazing by the euphausiid *Euphausia*
1250 *pacifica*? *J. Plankton Res.* 21, 2203–2217. <https://doi.org/10.1093/plankt/21.11.2203>

Formatted: German

Formatted: German

Formatted: German

- 1251 Penezić, A., Drozdowska, V., Novak, T., Gašparović, B., 2022. Distribution and characterization of organic matter within the
1252 sea surface microlayer in the Gulf of Gdańsk. *Oceanologia* 64, 631–650.
1253 <https://doi.org/10.1016/j.oceano.2022.05.003>
- 1254 Penna, A., 1999. Influence of nutrient ratios on the in vitro extracellular polysaccharide production by marine diatoms from
1255 the Adriatic Sea. *J. Plankton Res.* 21, 1681–1690. <https://doi.org/10.1093/plankt/21.9.1681>
- 1256 Pereira, R., Ashton, I., Sabbaghzadeh, B., Shutler, J.D., Upstill-Goddard, R.C., 2018. Reduced air–sea CO₂ exchange in the
1257 Atlantic Ocean due to biological surfactants. *Nat. Geosci.* 11, 492–496. <https://doi.org/10.1038/s41561-018-0136-2>
- 1258 Pereira, R., Schneider-Zapp, K., Upstill-Goddard, R.C., 2016. Surfactant control of gas transfer velocity along an offshore
1259 coastal transect: results from a laboratory gas exchange tank. *Biogeosciences* 13, 3981–3989.
1260 <https://doi.org/10.5194/bg-13-3981-2016>
- 1261 Petersen, M.K., Iyengar, S.S., Day, T.J.F., Voth, G.A., 2004. The Hydrated Proton at the Water Liquid/Vapor Interface. *J.*
1262 *Phys. Chem. B* 108, 14804–14806. <https://doi.org/10.1021/jp046716o>
- 1263 Pogorzelski, S.J., Kogut, A.D., Mazurek, A.Z., 2006. Surface Rheology Parameters of Source-Specific Surfactant Films as
1264 Indicators of Organic Matter Dynamics. *Hydrobiologia* 554, 67–81. <https://doi.org/10.1007/s10750-005-1007-6>
- 1265 Reinthaler, T., Sintès, E., Herndl, G.J., 2008. Dissolved organic matter and bacterial production and respiration in the sea-
1266 surface microlayer of the open Atlantic and the western Mediterranean Sea. *Limnol. Oceanogr.* 53, 122–136.
1267 <https://doi.org/10.4319/lo.2008.53.1.0122>
- 1268 Robinson, T., Wurl, O., Bahlmann, E., Jürgens, K., Stolle, C., 2019. Rising bubbles enhance the gelatinous nature of the air-
1269 sea interface. *Limnol. Oceanogr.* 64, 2358–2372. <https://doi.org/10.1002/lno.11188>
- 1270 Sabbaghzadeh, B., Upstill-Goddard, R.C., Beale, R., Pereira, R., Nightingale, P.D., 2017. The Atlantic Ocean surface
1271 microlayer from 50°N to 50°S is ubiquitously enriched in surfactants at wind speeds up to 13 m s⁻¹. *Geophys. Res.*
1272 *Lett.* 44, 2852–2858. <https://doi.org/10.1002/2017GL072988>
- 1273 Salter, M.E., Upstill-Goddard, R.C., Nightingale, P.D., Archer, S.D., Blomquist, B., Ho, D.T., Huebert, B., Schlosser, P.,
1274 Yang, M., 2011. Impact of an artificial surfactant release on air-sea gas fluxes during Deep Ocean Gas Exchange
1275 Experiment II. *J. Geophys. Res. Oceans* 116, 2011JC007023. <https://doi.org/10.1029/2011JC007023>
- 1276 Schartau, M., Engel, A., Schröter, J., Thoms, S., Völker, C., Wolf-Gladrow, D., 2007. Modelling carbon overconsumption and
1277 the formation of extracellular particulate organic carbon. *Biogeosciences* 4, 433–454. <https://doi.org/10.5194/bg-4-433-2007>
- 1278 Schartau, M., Landry, M.R., Armstrong, R.A., 2010. Density estimation of plankton size spectra: a reanalysis of IronEx II
1279 data. *J. Plankton Res.* 32, 1167–1184. <https://doi.org/10.1093/plankt/fbq072>
- 1280 Shine, J.P., Wallace, G.T., 1996. Flux of surface-active organic complexes of copper to the air-sea interface in coastal marine
1281 waters. *J. Geophys. Res. Oceans* 101, 12017–12026. <https://doi.org/10.1029/96JC00616>
- 1282 Sieburth, J.McN., 1983. Microbiological and Organic-Chemical Processes in the Surface and Mixed Layers, in: Liss, P.S.,
1283 Slinn, W.G.N. (Eds.), *Air-Sea Exchange of Gases and Particles*. Springer Netherlands, Dordrecht, pp. 121–172.
1284 https://doi.org/10.1007/978-94-009-7169-1_3
- 1285 Sieburth, J.McN., Willis, P.-J., Johnson, K.M., Burney, C.M., Lavoie, D.M., Hinga, K.R., Caron, D.A., French, F.W., Johnson,
1286 P.W., Davis, P.G., 1976. Dissolved Organic Matter and Heterotrophic Microneuston in the Surface Microlayers of
1287 the North Atlantic. *Science* 194, 1415–1418. <https://doi.org/10.1126/science.194.4272.1415>
- 1288 Silverman, B.W., 1986. *Density estimation for statistics and data analysis*. Chapman & Hall.
- 1289 Södergren, A., 1987. Origin and composition of surface slicks in lakes of differing trophic status I. *Limnol. Oceanogr.* 32,
1290 1307–1316. <https://doi.org/10.4319/lo.1987.32.6.1307>
- 1291 Springer, T.G., Pigford, R.L., 1970. Influence of Surface Turbulence and Surfactants on Gas Transport through Liquid
1292 Interfaces. *Ind. Eng. Chem. Fundam.* 9, 458–465. <https://doi.org/10.1021/i160035a025>
- 1293 Sun, C.-C., Sperling, M., Engel, A., 2018. Effect of wind speed on the size distribution of gel particles in the sea surface
1294 microlayer: insights from a wind-wave channel experiment. *Biogeosciences* 15, 3577–3589.
1295 <https://doi.org/10.5194/bg-15-3577-2018>
- 1296 Thornton, D.C.O., Brooks, S.D., Chen, J., 2016. Protein and Carbohydrate Exopolymer Particles in the Sea Surface Microlayer
1297 (SML). *Front. Mar. Sci.* 3. <https://doi.org/10.3389/fmars.2016.00135>
- 1298 Tsai, W., Liu, K., 2003. An assessment of the effect of sea surface surfactant on global atmosphere-ocean CO₂ flux. *J. Geophys.*
1299 *Res. Oceans* 108, 2000JC000740. <https://doi.org/10.1029/2000JC000740>
- 1300

Formatted: German

Formatted: German

- 1301 Tukey, J.W., 1977. Exploratory data analysis. Springer.
- 1302 Upstill-Goddard, R.C., 2006. Air–sea gas exchange in the coastal zone. *Estuar. Coast. Shelf Sci.* 70, 388–404.
1303 <https://doi.org/10.1016/j.ecss.2006.05.043>
- 1304 Verdugo, P., Alldredge, A.L., Azam, F., Kirchman, D.L., Passow, U., Santschi, P.H., 2004. The oceanic gel phase: a bridge in
1305 the DOM–POM continuum. *Mar. Chem.* 92, 67–85. <https://doi.org/10.1016/j.marchem.2004.06.017>
- 1306 Vitousek, P.M., 2004. Nutrient cycling and limitation: Hawai'i as a model system. Princeton University Press.
- 1307 Wegman, E.J., 1972. Nonparametric probability density estimation. *J. Stat. Comput. Simul.* 1, 225–245.
1308 <https://doi.org/10.1080/00949657208810017>
- 1309 Williams, P.M., Carlucci, A.F., Henrichs, S.M., Van Vleet, E.S., Horrigan, S.G., Reid, F.M.H., Robertson, K.J., 1986.
1310 Chemical and microbiological studies of sea-surface films in the Southern Gulf of California and off the West Coast
1311 of Baja California. *Mar. Chem.* 19, 17–98. [https://doi.org/10.1016/0304-4203\(86\)90033-2](https://doi.org/10.1016/0304-4203(86)90033-2)
- 1312 Wurl, O., Holmes, M., 2008. The gelatinous nature of the sea-surface microlayer. *Mar. Chem.* 110, 89–97.
1313 <https://doi.org/10.1016/j.marchem.2008.02.009>
- 1314 Wurl, O., Miller, L., Röttgers, R., Vagle, S., 2009. The distribution and fate of surface-active substances in the sea-surface
1315 microlayer and water column. *Mar. Chem.* 115, 1–9. <https://doi.org/10.1016/j.marchem.2009.04.007>
- 1316 Wurl, O., Stolle, C., Van Thuc, C., The Thu, P., Mari, X., 2016. Biofilm-like properties of the sea surface and predicted
1317 effects on air–sea CO₂ exchange. *Prog. Oceanogr.* 144, 15–24. <https://doi.org/10.1016/j.pocean.2016.03.002>
- 1318 Wurl, O., Wurl, E., Miller, L., Johnson, K., Vagle, S., 2011. Formation and global distribution of sea-surface microlayers.
1319 *Biogeosciences* 8, 121–135. <https://doi.org/10.5194/bg-8-121-2011>
- 1320 Yang, G.-P., 1999. Dimethylsulfide enrichment in the surface microlayer of the South China Sea. *Mar. Chem.* 66, 215–224.
1321 [https://doi.org/10.1016/S0304-4203\(99\)00042-0](https://doi.org/10.1016/S0304-4203(99)00042-0)
- 1322 Zhang, Z., Liu, C., Liu, L., 2006. Physicochemical Studies of the Sea-Surface Microlayer. *Front. Chem. China* 1.
1323 <https://doi.org/10.1007/s11458-005-0003-8>
- 1324 Zhou, J., Mopper, K., Passow, U., 1998. The role of surface-active carbohydrates in the formation of transparent exopolymer
1325 particles by bubble adsorption of seawater. *Limnol. Oceanogr.* 43, 1860–1871.
1326 <https://doi.org/10.4319/lo.1998.43.8.1860>
- 1327 Žutić, V., Cosović, B., Marčenko, E., Bihari, N., Kršinić, F., 1981. Surfactant production by marine phytoplankton. *Mar.*
1328 *Chem.* 10, 505–520. [https://doi.org/10.1016/0304-4203\(81\)90004-9](https://doi.org/10.1016/0304-4203(81)90004-9)
- 1329 Zuur, A.F., Ieno, E.N., Smith, G.M. (Eds.), 2007. Linear regression, in: *Analysing Ecological Data*. Springer New York, New
1330 York, NY, pp. 49–77. https://doi.org/10.1007/978-0-387-45972-1_5
- 1331

Formatted: German

▲ **Page 2: [1] Formatted** Amavi Silva 13/01/2026 10:41:00

Font colour: Text 2

▲ **Page 2: [2] Formatted** Amavi Silva 13/01/2026 10:41:00

Font colour: Text 2

▲ **Page 2: [3] Formatted** Amavi Silva 13/01/2026 10:41:00

Font colour: Text 2

▲ **Page 2: [4] Formatted** Amavi Silva 26/11/2025 11:49:00

Font colour: Text 2

▲ **Page 2: [5] Formatted** Amavi Silva 26/11/2025 11:49:00

Font colour: Text 2

▲ **Page 2: [6] Formatted** Amavi Silva 26/11/2025 11:49:00

Font colour: Text 2

▲ **Page 2: [7] Formatted** Amavi Silva 26/11/2025 11:49:00

Font colour: Text 2

▲ **Page 2: [8] Deleted** Amavi Silva 25/11/2025 09:56:00

✖

▲ **Page 2: [9] Formatted** Amavi Silva 26/11/2025 11:49:00

Font colour: Text 2

▲ **Page 2: [10] Formatted** Amavi Silva 26/11/2025 11:49:00

Font colour: Text 2, German

▲ **Page 2: [11] Deleted** Amavi Silva 25/11/2025 10:03:00

✖

▲ **Page 2: [12] Formatted** Amavi Silva 26/11/2025 11:49:00

Font colour: Text 2

▲ **Page 2: [13] Formatted** Amavi Silva 26/11/2025 11:49:00

Font colour: Text 2

▲ **Page 2: [14] Formatted** Amavi Silva 26/11/2025 11:49:00

Font colour: Text 2

▲ **Page 2: [15] Formatted** Amavi Silva 26/11/2025 11:49:00

Font colour: Text 2

▲ **Page 2: [16] Formatted** Amavi Silva 26/11/2025 11:49:00

Font colour: Text 2

▲

Page 2: [17] Deleted Amavi Silva 25/11/2025 10:14:00

x

Page 2: [18] Formatted Amavi Silva 26/11/2025 11:49:00

Font colour: Text 2

Page 2: [19] Formatted Amavi Silva 26/11/2025 11:49:00

Font colour: Text 2

Page 2: [20] Formatted Amavi Silva 25/11/2025 15:04:00

Suppress line numbers

Page 2: [21] Formatted Amavi Silva 14/01/2026 14:16:00

Font colour: Text 1

Page 2: [22] Formatted Amavi Silva 13/01/2026 11:04:00

Font colour: Text 2

Page 2: [23] Deleted Markus Schartau 30/01/2026 10:28:00

v

Page 2: [24] Formatted Amavi Silva 13/01/2026 10:46:00

Font: Italic

Page 2: [25] Formatted Amavi Silva 13/01/2026 10:59:00

Font colour: Text 2

Page 2: [26] Formatted Amavi Silva 13/01/2026 10:59:00

Font: Italic, Font colour: Text 2

Page 2: [27] Formatted Amavi Silva 13/01/2026 10:59:00

Font colour: Text 2

Page 2: [28] Formatted Amavi Silva 13/01/2026 10:59:00

Font: Italic, Font colour: Text 2

Page 2: [29] Formatted Amavi Silva 13/01/2026 10:59:00

Font colour: Text 2

Page 5: [30] Deleted Amavi Silva 25/11/2025 12:54:00

x

Page 5: [31] Deleted Amavi Silva 25/11/2025 12:46:00

x

Page 5: [32] Deleted Amavi Silva 25/11/2025 15:45:00

Page 5: [33] Formatted Markus Schartau 30/01/2026 11:10:00

Font: (Default) Times New Roman, Font colour: Auto

▲
Page 18: [34] Formatted Amavi Silva 26/01/2026 17:10:00

Font: (Default) Times New Roman, 10 pt, Font colour: Text 2, English (US)

▲
Page 18: [35] Formatted Amavi Silva 26/01/2026 17:15:00

Font: (Default) Times New Roman, 10 pt, Font colour: Text 2, English (US)

▲
Page 18: [36] Deleted Amavi Silva 10/12/2025 17:10:00

✖

▲
Page 21: [37] Formatted Amavi Silva 13/01/2026 11:16:00

Font colour: Text 2

▲
Page 21: [37] Formatted Amavi Silva 13/01/2026 11:16:00

Font colour: Text 2

▲
Page 21: [38] Deleted Amavi Silva 11/12/2025 17:32:00

✖

▲
Page 21: [38] Deleted Amavi Silva 11/12/2025 17:32:00

✖

▲
Page 21: [39] Formatted Amavi Silva 26/01/2026 17:32:00

Font: (Default) Times New Roman, 10 pt, Font colour: Text 2, English (US)

▲
Page 21: [39] Formatted Amavi Silva 26/01/2026 17:32:00

Font: (Default) Times New Roman, 10 pt, Font colour: Text 2, English (US)

▲
Page 21: [39] Formatted Amavi Silva 26/01/2026 17:32:00

Font: (Default) Times New Roman, 10 pt, Font colour: Text 2, English (US)

▲
Page 21: [39] Formatted Amavi Silva 26/01/2026 17:32:00

Font: (Default) Times New Roman, 10 pt, Font colour: Text 2, English (US)

▲
Page 21: [39] Formatted Amavi Silva 26/01/2026 17:32:00

Font: (Default) Times New Roman, 10 pt, Font colour: Text 2, English (US)

▲
Page 21: [39] Formatted Amavi Silva 26/01/2026 17:32:00

Font: (Default) Times New Roman, 10 pt, Font colour: Text 2, English (US)

▲
Page 21: [39] Formatted Amavi Silva 26/01/2026 17:32:00

Font: (Default) Times New Roman, 10 pt, Font colour: Text 2, English (US)

▲
Page 21: [39] Formatted Amavi Silva 26/01/2026 17:32:00

Font: (Default) Times New Roman, 10 pt, Font colour: Text 2, English (US)

▲
Page 21: [39] Formatted Amavi Silva 26/01/2026 17:32:00

Font: (Default) Times New Roman, 10 pt, Font colour: Text 2, English (US)

▲
Page 21: [39] Formatted Amavi Silva 26/01/2026 17:32:00

Font: (Default) Times New Roman, 10 pt, Font colour: Text 2, English (US)

▲
Page 21: [39] Formatted Amavi Silva 26/01/2026 17:32:00

Font: (Default) Times New Roman, 10 pt, Font colour: Text 2, English (US)

▲
Page 21: [40] Formatted Amavi Silva 27/01/2026 13:23:00

Font: (Default) Times New Roman, 10 pt, Font colour: Text 2, English (US)

▲
Page 21: [40] Formatted Amavi Silva 27/01/2026 13:23:00

Font: (Default) Times New Roman, 10 pt, Font colour: Text 2, English (US)

▲
Page 21: [40] Formatted Amavi Silva 27/01/2026 13:23:00

Font: (Default) Times New Roman, 10 pt, Font colour: Text 2, English (US)

▲
Page 21: [41] Formatted Amavi Silva 13/01/2026 13:34:00

Font colour: Text 1

▲
Page 21: [41] Formatted Amavi Silva 13/01/2026 13:34:00

Font colour: Text 1

▲
Page 21: [41] Formatted Amavi Silva 13/01/2026 13:34:00

Font colour: Text 1

▲
Page 21: [41] Formatted Amavi Silva 13/01/2026 13:34:00

Font colour: Text 1

▲
Page 21: [41] Formatted Amavi Silva 13/01/2026 13:34:00

Font colour: Text 1

▲
Page 21: [41] Formatted Amavi Silva 13/01/2026 13:34:00

Font colour: Text 1

▲
Page 21: [41] Formatted Amavi Silva 13/01/2026 13:34:00

Font colour: Text 1

▲
Page 21: [41] Formatted Amavi Silva 13/01/2026 13:34:00

Font colour: Text 1

▲
Page 21: [42] Formatted Amavi Silva 13/01/2026 11:17:00

Font colour: Text 2

▲
Page 21: [42] Formatted Amavi Silva 13/01/2026 11:17:00

Font colour: Text 2

▲
Page 21: [43] Formatted Amavi Silva 13/01/2026 11:17:00

Font colour: Text 2

▲
Page 21: [43] Formatted Amavi Silva 13/01/2026 11:17:00

Font colour: Text 2

▲
Page 21: [43] Formatted Amavi Silva 13/01/2026 11:17:00

Font colour: Text 2

▲
Page 21: [43] Formatted Amavi Silva 13/01/2026 11:17:00

Font colour: Text 2

▲
Page 21: [44] Formatted Amavi Silva 13/01/2026 13:34:00

Font colour: Text 1

▲
Page 21: [44] Formatted Amavi Silva 13/01/2026 13:34:00

Font colour: Text 1

▲
Page 21: [45] Formatted Amavi Silva 13/01/2026 11:17:00

Font colour: Text 2

▲
Page 21: [45] Formatted Amavi Silva 13/01/2026 11:17:00

Font colour: Text 2

▲
Page 21: [45] Formatted Amavi Silva 13/01/2026 11:17:00

Font colour: Text 2

▲
Page 21: [46] Formatted Amavi Silva 13/01/2026 11:17:00

Font colour: Text 2

▲
Page 21: [46] Formatted Amavi Silva 13/01/2026 11:17:00

Font colour: Text 2

▲
Page 21: [46] Formatted Amavi Silva 13/01/2026 11:17:00

Font colour: Text 2

▲
Page 21: [46] Formatted Amavi Silva 13/01/2026 11:17:00

Font colour: Text 2

▲
Page 21: [46] Formatted Amavi Silva 13/01/2026 11:17:00

Font colour: Text 2

▲
Page 21: [46] Formatted Amavi Silva 13/01/2026 11:17:00

Font colour: Text 2

▲
Page 21: [47] Formatted Amavi Silva 13/01/2026 11:17:00

Font colour: Text 2

▲
Page 21: [47] Formatted Amavi Silva 13/01/2026 11:17:00

Font colour: Text 2

▲
Page 21: [47] Formatted Amavi Silva 13/01/2026 11:17:00

Font colour: Text 2

▲
Page 21: [47] Formatted Amavi Silva 13/01/2026 11:17:00

Font colour: Text 2

▲
Page 21: [47] Formatted Amavi Silva 13/01/2026 11:17:00

Font colour: Text 2

▲
Page 21: [47] Formatted Amavi Silva 13/01/2026 11:17:00

Font colour: Text 2

▲
Page 21: [47] Formatted Amavi Silva 13/01/2026 11:17:00

Font colour: Text 2

▲
Page 21: [47] Formatted Amavi Silva 13/01/2026 11:17:00

Font colour: Text 2

▲
Page 21: [47] Formatted Amavi Silva 13/01/2026 11:17:00

Font colour: Text 2

▲
Page 21: [47] Formatted Amavi Silva 13/01/2026 11:17:00

Font colour: Text 2

▲
Page 21: [47] Formatted Amavi Silva 13/01/2026 11:17:00

Font colour: Text 2

▲
Page 21: [47] Formatted Amavi Silva 13/01/2026 11:17:00

Font colour: Text 2

▲
Page 21: [47] Formatted Amavi Silva 13/01/2026 11:17:00

Font colour: Text 2

▲
Page 21: [47] Formatted Amavi Silva 13/01/2026 11:17:00

Font colour: Text 2

▲
Page 21: [47] Formatted Amavi Silva 13/01/2026 11:17:00

Font colour: Text 2

▲
Page 21: [47] Formatted Amavi Silva 13/01/2026 11:17:00

Font colour: Text 2

▲
Page 21: [47] Formatted Amavi Silva 13/01/2026 11:17:00

Font colour: Text 2

▲
Page 21: [47] Formatted Amavi Silva 13/01/2026 11:17:00

Font colour: Text 2

▲
Page 21: [48] Formatted Amavi Silva 13/01/2026 11:17:00

Font colour: Text 2

▲
Page 21: [48] Formatted Amavi Silva 13/01/2026 11:17:00

Font colour: Text 2

▲
Page 21: [48] Formatted Amavi Silva 13/01/2026 11:17:00

Font colour: Text 2

▲
Page 21: [48] Formatted Amavi Silva 13/01/2026 11:17:00

Font colour: Text 2

▲
Page 21: [48] Formatted Amavi Silva 13/01/2026 11:17:00

Font colour: Text 2

▲
Page 21: [48] Formatted Amavi Silva 13/01/2026 11:17:00

Font colour: Text 2

▲